https://doi.org/10.5194/os-2020-76
Preprint. Discussion started: 18 August 2020

Ocean Science
Discussions
Open Access
EGU

The Atlantic's Freshwater Budget under Climate Change in the Community Earth System Model with Strongly Eddying Oceans

André Jüling[1], Xun Zhang[1], Daniele Castellana[1], Anna S. von der Heydt[1], and Henk A. Dijkstra[1]

[1]Institute for Marine and Atmospheric research Utrecht (IMAU), Utrecht University, Netherlands

Correspondence: André Jüling (a.juling@uu.nl)

Abstract. We investigate the freshwater and salinity budget of the Atlantic and Arctic oceans in a strongly eddying coupled climate change simulation with the Community Earth System Model (CESM) and compare it to a simulation with a coarse ocean resolution CESM configuration, typical of CMIP6 models. Details of these budgets are important to understand the evolution of the Atlantic Meridional Overturning Circulation (AMOC) under climate change. We find that the slowdown of the AMOC in 2100 under the increasing CO_2 concentrations of the RCP8.5 scenario is almost identical between both simulations. Also, the surface freshwater fluxes are similar in their mean and trend under climate change in both simulations. While the basin-scale total freshwater transport is similar between the simulations, significant local differences exist. The high ocean resolution simulation exhibits significantly reduced ocean state biases, notably in the salt distribution, due to an improved circulation. Mesoscale eddies contribute considerably to the freshwater and salt transport, in particular at the boundary of the subtropical and subpolar gyres. Both simulations start in the single equilibrium AMOC regime according to a commonly used AMOC stability indicator and evolve towards the multiple equilibrium regime under climate change, but only the high resolution simulation enters it due to the reduced biases in the freshwater budget.

Keywords. Atlantic Meridional Overturning Circulation
Mesoscale ocean flows
Climate Change
Ocean freshwater transports
Freshwater budget

https://doi.org/10.5194/os-2020-76
Preprint. Discussion started: 18 August 2020

Ocean Science
Discussions
Open Access
EGU

1 Introduction

One of the important Tipping Elements in the climate system (Lenton et al., 2008) is the Atlantic Meridional Overturning Circulation (AMOC). This component of the ocean circulation carries about 1.5 PW of heat northwards (Johns et al., 2011) at 26.5°N in the Atlantic and hence its strength and spatial expression significantly affect local surface temperature and precipitation (Palter, 2015). The potential tipping character of the AMOC is expressed through large and abrupt changes in AMOC strength (Srokosz et al., 2012; Weijer et al., 2019), for which evidence exists in the palaeo record (Lynch-Stieglitz, 2017). In models of the AMOC, such transitions can occur due to the existence of multiple equilibria, where several AMOC states can coexist under the same forcing conditions. Such multiple equilibria of the AMOC have been found in a hierarchy of ocean-climate models (Stommel, 1961; Rahmstorf et al., 2005; Hawkins et al., 2011; Toom et al., 2012). They occur due to the presence of positive feedbacks, the most prominent one being the salt-advection feedback. Subtle changes to the freshwater budget can modify the AMOC response to perturbations which is why the correct simulation of the oceanic freshwater budget in the Arctic and Atlantic is important.

The Atlantic is a net evaporative basin resulting in the saltiest subtropical surface waters of all the major oceans. At the Atlantic's southern boundary, which we take to coincide with the southern tip of Africa at 34°S, relatively salty surface waters together with fresh Antarctic Intermediate Waters are imported in the upper kilometer and this transport amounts to some 17 Sv at 26.5°N. At high northern latitudes the surface waters are transformed into North Atlantic Deep Water (NADW) which returns southwards and is exported at 34°S. A lower, weaker overturning cell exists in which cold Antarctic Bottom Water enters the South Atlantic at the bottom and returns just above with the NADW. Salt also enters the South Atlantic from the Southwest Indian Ocean via Agulhas leakage in the form of eddies shed off the Agulhas retroflection (McDonagh et al., 1999). From the North, some 0.8 Sv of relatively fresh Pacific water enters the Arctic Ocean via Bering Strait where it further freshens primarily due to river discharge from the large Arctic catchment area. Together with freshwater in the form of sea ice, relatively fresh seawater enters the Atlantic from the North. Freshwater is also exchanged with the Mediterranean Sea which is strongly evaporative. The meridional asymmetry of the precipitation pattern of the Intertropical Convergence Zone (ITCZ) results in salinity differences between the North and South Atlantic. The wind driven subtropical and subpolar gyres recirculate water primarily horizontally and advect salt meridionally when there is a zonal salinity gradient.

As atmospheric temperatures rise under greenhouse gas increases, the hydrological cycle generally strengthens making dry regions drier and wet regions wetter, amplifying sea surface salinity patterns (Held and Soden, 2006; Skliris et al., 2020). The AMOC is projected to weaken under climate change due to buoyancy flux changes as net precipitation patterns change (Stocker et al., 2013) and there is evidence that the AMOC strength reduction is already underway (Caesar et al., 2018). In order to judge how fast the AMOC can change and whether it could collapse abruptly, one needs to assess the AMOC stability and in particular the strength of the positive feedbacks. In CMIP5 models, no transition to a different statistical equilibrium state is found up to the year 2100 under any of the climate change scenarios (Cheng et al., 2013) and it remains unclear whether the AMOC is already in or will shift into a multiple equilibrium regime, which would allow such transitions (Gent, 2018).

https://doi.org/10.5194/os-2020-76
Preprint. Discussion started: 18 August 2020


Ocean Science
Discussions
Open Access
EGU

Many studies have linked the freshwater budget, through the salt-advection feedback, to the response of the AMOC under surface freshwater perturbations (Rahmstorf, 1996; de Vries, 2005; Dijkstra, 2007; Mecking et al., 2017; Liu et al., 2017). The existence of a multiple equilibrium regime is connected to the sign of the divergence of the advective AMOC induced Atlantic freshwater transport Σ (or ΔM_{ov} in Liu et al. (2017)) which exactly marks the separation of the unique and multiple equilibrium regimes when atmospheric feedbacks are negligible (Dijkstra, 2007). As the northern boundary freshwater transport is minor this divergence is often approximated by its southern boundary component only, referred to M_{ov} (de Vries, 2005), F_{ov} (Hawkins et al., 2011) or F_{ovS} (Weijer et al., 2019). We will use F_{ovS} here as we use F to denote freshwater fluxes in general and F_{ov} for the latitudinally dependend overturning component in particular. Positive F_{ovS} values indicate that the AMOC imports freshwater which constitutes a negative feedback as a positive AMOC strength perturbation would be damped by an enhanced freshwater import into the North Atlantic suppressing deep water formation. A negative F_{ovS} value, on the other hand, would induce an amplification of an AMOC perturbation (Huisman et al., 2010). Observational estimates of F_{ovS} are negative suggesting multiple AMOC equilibria in the present-day climate (Weijer et al., 2019). The models of the last two model intercomparison projects CMIP3 and CMIP5 tend to have positive F_{ovS} values due to a bias in the salinity at 34°S where the upper water masses are too fresh and the deep southward return flow is too salty (Drijfhout et al., 2011; Mecking et al., 2017). Once this bias is accounted for, F_{ovS} values for most models lie within the range of observations (Mecking et al., 2017). Under climate change, CMIP3 models exhibit a negative F_{ovS} trend.

Refining the grid spacing from 1° typical of CMIP5 and CMIP6 ocean model components to 0.1° resolves the internal Rossby radius of deformation over large parts of the ocean (Hallberg, 2013). This enables the development of eddies, filaments, and fronts through mixed barotropic/baroclinic instabilities and the simulation of other mesoscale ocean features such as currents at the western boundary and through narrow straits. We use the terminology “strongly eddying" for ocean grids with 0.1° horizontal grid spacing as these are neither just eddy-permitting (typically 0.25°) nor fully mesoscale turbulence (Moreton et al., 2020). These high resolution ocean models constitute the only consistent method to estimate eddy contributions to ocean variability and the mean climate state and generally result in significantly reduced ocean biases (Kirtman et al., 2012; Small et al., 2014). The eddy freshwater transport is comparable in magnitude to the mean transport at the poleward and equatorward boundaries of the subtropical gyres (Treguier et al., 2012, 2014). Some of this transport will be captured by eddy parametrizations in low resolution simulation, but other effects, such as the advection of salt by Agulhas Rings, cannot be captured adequately.

Relatively few studies have investigated the AMOC behavior in strongly eddying ocean models (Weijer et al., 2012; den Toom et al., 2014; Brunnabend and Dijkstra, 2017; Hirschi et al., 2020). The improved simulation of overflows over sills in high resolution models significantly reduces deep water density biases which leads to improved simulation of deep convection. The pathway of the North Atlantic Current and the formation sites of North Atlantic Deep Water are more realistic at high resolution (Hirschi et al., 2020). A comparison of the AMOC response between 10 GFDL models under a 1% per year CO_2 increase scenario showed that in coarse resolution models, the AMOC declines between 16% and 45%, and the eddy-permitting and strongly-eddying configurations are at the lower end of these percentages with 13% and 16%, respectively (Winton et al., 2014). The POP ocean model showed qualitatively similar AMOC responses to surface freshwater perturbations between

https://doi.org/10.5194/os-2020-76
Preprint. Discussion started: 18 August 2020


Ocean Science Discussions

strongly eddying ($0.1°$) and non-eddying ($1°$) model configurations (Weijer et al., 2012; den Toom et al., 2014; Brunnabend and Dijkstra, 2017), but with a dependence on the location of the perturbation. However, whether ocean model resolution affects the AMOC response to forcing systematically remains an open question (Gent, 2018). A suite of high resolution ocean hindcasts with the NEMO model at $1/12°$ show that the stability indicator F_{ovS} is negative (Deshayes et al., 2013) in contrast to coarse resolution models (Mecking et al., 2017).

As coarse resolution models exhibit biases in their mean state and lack mesoscale processes, the simulated sensitivity to forcing may be inadequate and the strength of the salt advection feedback may be affected. We investigate the effect of improving the ocean model resolution on the Atlantic freshwater budget and its sensitivity by analyzing present day control and high CO_2 concentration pathway simulations in two configurations of the Community Earth System Model (CESM), one with a nominal horizontal resolution in the ocean model of $0.1°$ and the other with $1°$. The following section 2 describes these model simulations and provides a model-observation comparison of the control simulations. Section 3 presents the results, including changes to the AMOC, the Atlantic freshwater and salt budgets, and the effects on AMOC stability, under the climate change scenario. The results are summarized and discussed in section 4.

2 Model simulations and model-observation comparison

2.1 CESM simulations

We analyze four simulations with the Community Earth System Model version 1 (CESM, Hurrell et al. (2013)), carried out at the Academic Computing Center in Amsterdam (SURFsara), see e.g. van Westen and Dijkstra (2017). The CESM components are CAM5 (Community Atmosphere Model), POP2 (Parallel Ocean Program), CICE (sea ice model), and CLM (Community Land Model) which are coupled by the CESM1 coupler. The ocean model formulation is volume conserving and surface freshwater fluxes are thus modeled as virtual salt fluxes. Tracer diffusing subgrid-scale processes are parameterized by the Gent-McWilliams scheme (Gent and McWilliams, 1990) in the $1°$ resolution simulation and by biharmonic diffusion in the $0.1°$ resolution case, which is strongly eddying over large parts of the ocean.

The high resolution (HIGH) simulation was performed with a $0.1°$ ocean horizontal grid spacing on a tripolar grid, while the low resolution (LOW) simulation was conducted with $1°$ ocean horizontal grid spacing with a displaced dipole grid. Both control simulations use constant year 2000 atmospheric greenhouse gas concentrations forcing (notably $[CO_2] = 367\,\mathrm{ppm}$, $[CH_4] = 1760\,\mathrm{ppb}$). The climate change simulations are following the CO_2 concentration of the highest Representative Concentration Pathway (RCP8.5) of the Coupled Model Intercomparison Project phase 5 (CMIP5) used in the Fifth Assessment Report of the Intergovernmental Panel on Climate Change (Stocker et al., 2013), but do not include other greenhouse gas increases or land use changes. We name the present-day control simulation CTRL and the climate change simulation RCP. The main characteristics of the model simulations are summarized in Table 1.

There are additional differences between the model configurations apart from the horizontal ocean model resolution. The POP2 model grids have 42 levels in the HIGH simulation and 60 levels in the LOW simulation, but the effects of this difference are hard to disentangle as the horizontal mixing is represented very differently. Further, the CESM versions and atmosphere

https://doi.org/10.5194/os-2020-76
Preprint. Discussion started: 18 August 2020


Ocean Science Discussions

Table 1. Overview of the CESM simulations used, their ocean and atmosphere grid, the model version, as well as the year at which the RCP simulations are branched off the CTRL simulations.

name	ocean grid	atmosphere grid	CESM version	begin RCP [year]
HIGH	0.1° tripole, 42 levels to 6000 m (`tx0.1v2`)	$0.47^\circ \times 0.63^\circ$ (`f05`)	1.04	200
LOW	1° dipole, 60 levels to 5500 m (`gx1v6`)	$0.9^\circ \times 1.25^\circ$ (`f09`)	1.12	500

resolution differ between the HIGH (version 1.04) and the LOW simulation (version 1.12). The newer version employs a different dynamical core in the atmosphere model (CAM5.2 versus CAM5.0) and some parameterization schemes are updated. In contrast to the improvement in ocean model resolution however, halving the atmospheric grid spacing from 1° to 0.5° is not resolving new essential physical processes. Therefore, no significant changes are expected between the 0.5° CAM5.0 HIGH and 1° CAM5.2 LOW atmospheres due their resolved physics apart from coupling to different ocean boundary conditions.

2.2 Model-observation comparison

To assess the performance of the HIGH and LOW CTRL simulations we use several observational datasets which are relevant for the freshwater budget and compare 30-year means of the CTRL simulations following the RCP branch-off point (years 200-229 and 500-529, see Tbl. 1). In many aspects the HIGH CTRL simulation performs better than the LOW CTRL simulation when compared to the present-day climate. Global maps of the quantities presented here for the Atlantic-Arctic and additional sea ice comparison results are included in Appendix A.

We define regions in the Atlantic that approximately correspond to the subtropical gyres (STG; sometimes specified as South or North Atlantic: SA-STG and NA-STG), subpolar gyre (SPG), the Intertropical Convergence Zone (ITCZ), and the Arctic. Figure 1 shows the bounding latitudes which are at the southern end of the Atlantic basin around 34°S, 10°S and 10°N generously bounding the ITCZ, 45°N as the approximate boundary of the subtropical and subpolar gyres, and 60°N as the boundary between the Atlantic and the Arctic. The Arctic Ocean includes Hudson Bay and is bounded on the Pacific side by the Bering Strait at 68°N. We perform the calculations on the original model 0.1° and 1° grids which become distorted relative to a regular latitude-longitude grid at high northern latitudes (see 60°N line in Fig. 1).

2.2.1 Sea surface temperature

The sea surface temperature (SST) is important for the freshwater budget as it strongly controls evaporation. Figure 1 shows the HadISST 1990-2019 SST climatology, the bias of the CTRL simulations with respect to that climatology, and the linear SST trends of the RCP simulations. The HIGH (LOW) simulation's global mean SST is about 0.51(0.86) K too warm with a RMSE of 0.99(1.39) K compared to the HadISST dataset. Some warm bias is to be expected as the simulations are subjected to constant year 2000 radiative forcing and not the transiently increasing historical forcing. In the HIGH Atlantic, with the exception of the South Atlantic near the African coast the sea surface is slightly too cold equatorward of 30° and too warm poleward of these latitudes. The LOW SST biases are stronger with warm biases in the South Atlantic, along the North American East Coast due

https://doi.org/10.5194/os-2020-76
Preprint. Discussion started: 18 August 2020

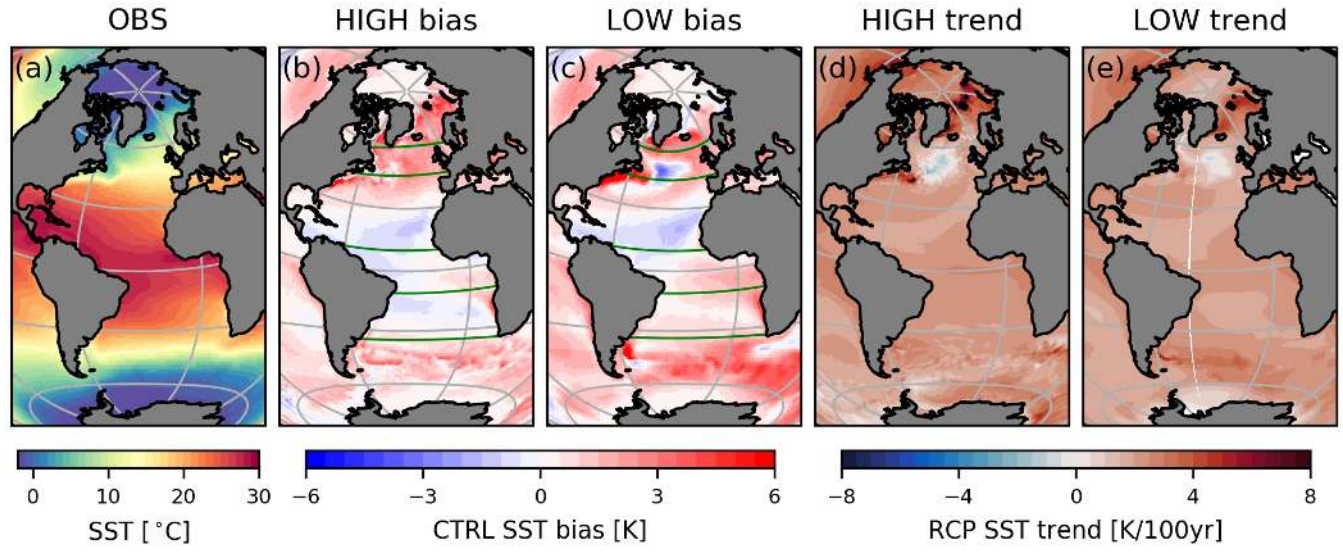

Figure 1. The sea surface temperature (SST) from the HadISST 1990-2019 observations (a), the SST bias of the HIGH (b) and LOW (c) CTRL simulations, and the linear trends of the HIGH (d) and LOW (e) RCP climate change scenarios. The Lambert Azimuthal projection of these and subsequent maps is an equal area projection and grey parallels (meridians) are drawn every 30° (60°). The green lines show transects in the tripolar HIGH and dipolar LOW model grid at 34°S, 10°S, 10°N, and approximately 45°N and 60°N. This northernmost meridional boundary differs from the 60°N parallel because of the curvilinear grids and is chosen to lie south of Hudson Strait.

to the Gulf Stream separating too far north, and north of 50°N. The LOW NA-STG and the southern edge of the NA-SPG are too cold resulting in asymmetric bias about the equator. Both simulations SSTs are too high in the NADW formation areas which results in warm biases in this water mass. The RCP SST trends are positive everywhere, except for the NA-SPG, and the positive trend is amplified in the Arctic.

2.2.2 Surface freshwater fluxes

We compare surface freshwater fluxes to ERA-Interim precipitation minus evaporation, $P-E$, 1989-2010 climatology (Dee et al., 2011; Trenberth et al., 2011). Figure 2 shows maps of the observed mean $P-E$ and the bias of the two simulations, and the zonally integrated $P-E$ fluxes. There is net evaporation in the STGs and net precipitation in the ITCZ just north of the equator (Fig. 2a) colocated with the maximum SSTs (cf. Fig. 1a) and the mid- to high-latitudes. Both simulations exhibit the same positive global precipitation biases of 0.23 ± 1.01 mm/day (mean±RMSE; see appendix A). The $P-E$ bias is negative almost everywhere in the HIGH Atlantic (Fig. 2b) and over large parts of the LOW Atlantic (Fig. 2c). Both simulations show biases around the ITZC, most noticeably with reduced precipitation near the South American coast north of the equator. The HIGH ITCZ appears slightly rotated with a wider precipitation belt in the central equatorial Atlantic and reduced precipitation in the Northwest and Southeast. The LOW ITCZ is shifted south because the SST bias (cf. Fig. 1c) is meridionally asymmetric

https://doi.org/10.5194/os-2020-76
Preprint. Discussion started: 18 August 2020

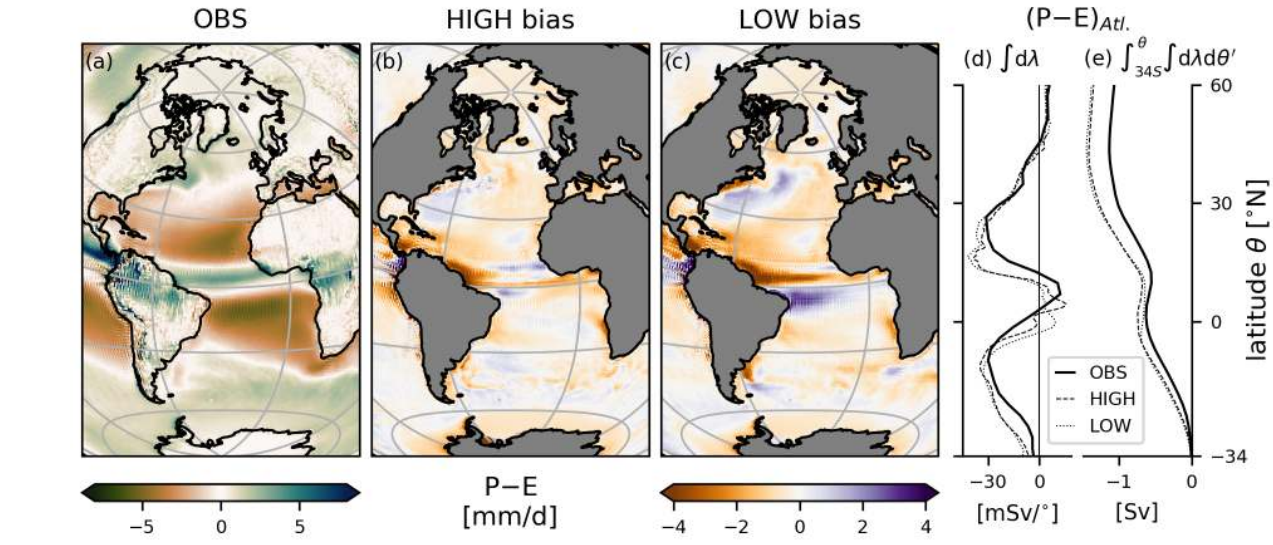

Figure 2. Precipitation minus evaporation: the observed ERA-Interim 1980-2010 climatology (a), and the biases of the CTRL HIGH (b) and LOW (c) simulations. The zonally integrated P-E fluxes per degree latitude (d) and the implied freshwater transports due to the P-E fluxes (e) assuming zero transport at 34°S and constant salt content in the oceans.

about the equator. Around the Gulf Stream too much water evaporates, but this is stronger and extends further north in the LOW simulation. The $P-E$ biases around the Gulf Stream reflect the SST biases there (cf. Fig. 1c). As the surface waters diverge at the equator this contributes to the saline (fresh) surface bias of the North (South) Atlantic. Both the flux per degree latitude and the meridionally integrated flux referenced to zero transport at 34°S reveal comparable biases (Fig. 2d) in the zonal integrals with minor differences in the ITCZ.

2.2.3 Salinity distribution

The circulation rearranges the salt imported from Bering Strait and the freshwater exchanged at the surface and with the Mediterranean resulting in a heterogeneous distribution of salt. We use the EN4 global salinity observations averaged over 1990-2019 which is provided on a $1 \times 1°$ grid (Good et al., 2013). To compare to the model data, we first interpolated the EN4 data bilinearly horizontally and then linearly to the model depth coordinates for both HIGH and LOW ocean grids. Figure 3 shows the observed salinity distribution and the simulation biases of the upper 100 m, as an Atlantic zonal mean, and along a zonal transect at 34°S. Both the HIGH (Fig. 3b) and LOW (Fig. 3c) simulations show a similar bias pattern with a positive surface bias in the North Atlantic and parts of the Arctic, and a negative bias in the South Atlantic and the rest of the global ocean (not shown). The Atlantic zonally averaged profile (Fig. 3d) and the 34°S transect (Fig. 3g) show the largest salinity values in the evaporative subtropical gyres with less saline waters of the NADW with $S = 34.9-35.0$ at high northern latitudes and between 1.5 and 4 km, while relatively fresh AAIW is visible around 1 km depth up to 20°N (Fig. 3j) The bias in the HIGH

https://doi.org/10.5194/os-2020-76
Preprint. Discussion started: 18 August 2020

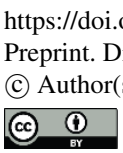

Ocean Science
Discussions
Open Access
EGU

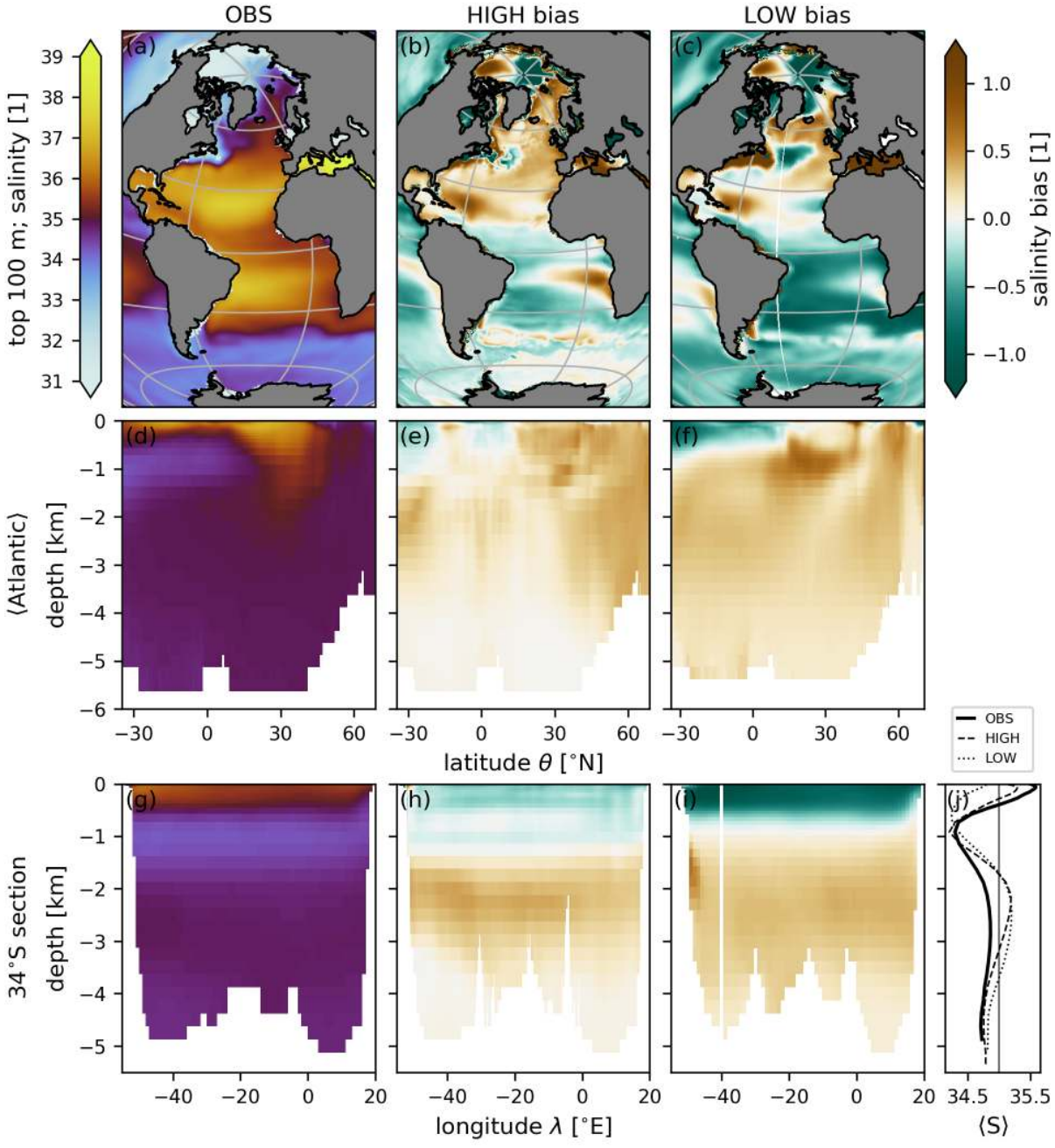

Figure 3. The salinity distribution in the EN4 observations (left) and the bias of the HIGH (center) and LOW (right) CTRL simulations for the top 100 m (top), zonally averaged in the Atlantic (middle), and at the 34°S transect (bottom). Panel (j) shows zonally averaged salinity profiles for observations (thick solid line) and the HIGH (dashed) and LOW (dotted) simulations together with the reference salinity $S_0 = 35$ (thin solid). Note that salinity as a mass fraction is dimensionless.

https://doi.org/10.5194/os-2020-76
Preprint. Discussion started: 18 August 2020

Ocean Science
Discussions
Open Access
EGU

simulation is significantly reduced compared the LOW simulation in all three planes. In particular, the LOW bias around 1 km depth and 15-30°N (Fig. 3f,i) can be attributed to the absence of eddies (Treguier et al., 2014).

2.2.4 Circulation and gateway transports

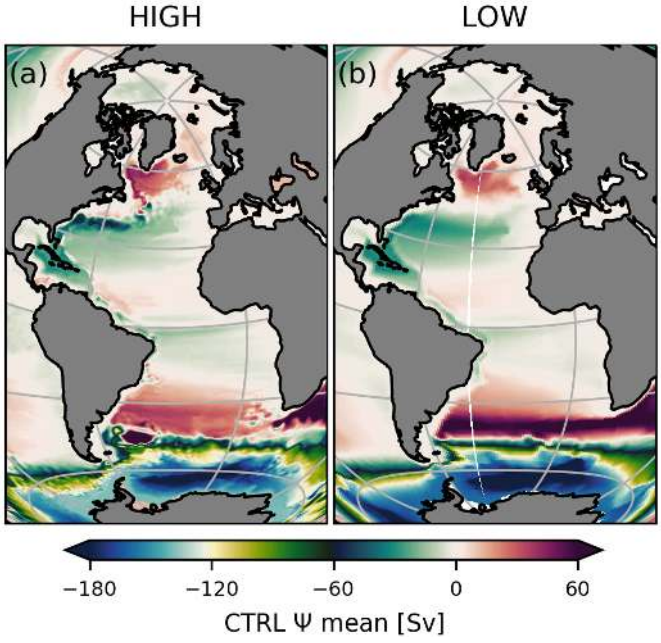

Figure 4. The mean barotropic streamfunction Ψ of the CTRL HIGH (a) and LOW (b) simulations relative to the African Atlantic coast.

To explain several of the HIGH and LOW salinity distribution biases, we plot the barotropic streamfunction for both CTRL cases in Fig. 4. An approximation of the barotropic streamfunction Ψ has been computed as $\Psi(\lambda,\theta) = \int_{\theta'=\theta_S}^{\theta}\int_{z=-D}^{0} u(\lambda,\theta',z)\,\mathrm{d}z\,\mathrm{d}\theta' - \Psi_0$. Here the vertical integral of the zonal velocity u is taken over the full depth from $z=-D$ to the surface $z=0$, the meridional integral is taken from the southern boundary at Antarctica $\theta=\theta_S$, and is subsequently set to 0 at the African Atlantic coast by removing a constant Ψ_0.

While the broad scale wind-driven subtropical and subpolar gyre circulation are present in both simulations, the HIGH simulation features stronger boundary currents, standing eddies, a more realistic Agulhas retroflection pathway and Gulf Stream separation point, and a stronger subpolar gyre which extends much further south along the North American coast. In the LOW simulation, the inflow of Indian Ocean waters is unrealistically strong and together with the strong upper 100 m fresh bias of the Indian Ocean (supplementary Fig. A3)) contribute to the negative salinity bias of the South Atlantic (Fig. 3). In the RCP scenario the Gulf Stream in the HIGH simulation shifts northward (not shown). In the LOW simulation the subpolar gyre weakens broadly, while in the HIGH simulation only the boundary currents weaken.

https://doi.org/10.5194/os-2020-76
Preprint. Discussion started: 18 August 2020


Ocean Science
Discussions
Open Access
EGU

190 The freshwater fraction W, which we call freshwater for brevity, is defined relative to a reference salinity S_0 as $W = (S - S_0)/S_0$ where S is the (dimensionless) salinity of a given ocean water parcel. We choose $S_0 = 35$ as this is the salinity of North Atlantic Deep Water and close to the average salinity at 34°S (cf. Figs. 3d/g/j). In principle, the freshwater framework has disadvantages, as the choice of the reference salinity S_0 is arbitrary and the amount of freshwater depends non-linearly on it (Schauer and Losch, 2019). However, the relevant terms relate to recirculating and eddy flows which are independent of S_0
195 (see App. B) and the AMOC stability criterion F_{ovS} is framed in terms of freshwater. Only the barotropic transport depends on S_0 and this component is negligible for the Atlantic freshwater transport although it contributes significantly to the total salt transport.

Table 2. Transports of sea water, salt, and freshwater through the Strait of Gibraltar and Bering Strait. The ± denotes uncertainties in the observations, and inter-annual standard deviations in the simulations.

strait	quantity	units	OBS	HIGH	LOW
Gibraltar	barotropic transport	[Sv]	0.038 ± 0.007	0	0
	overturning	[Sv]	0.8	−	−
	salt transport	[kt/s]	0	-1.2 ± 0.1	-1.2 ± 0.1
	FW transport	[Sv]	0.05	0.032 ± 0.002	0.032 ± 0.002
Bering	barotropic transport	[Sv]	0.8 ± 0.1	1.6 ± 0.1	1.0 ± 0.1
	salt transport	[kt/s]	26 ± 3	51 ± 4	32 ± 1
	FW transport	[Sv]	0.14 ± 0.02	0.10 ± 0.03	0.10 ± 0.03

For the Atlantic-Arctic basin the only oceanic exchanges of freshwater and salt north of 34°S occurs at Bering Strait with the Pacific Ocean and through the Strait of Gibraltar with the Mediterranean Sea. Table 2 summarizes the observed and simulated
200 transports of sea water, salt, and freshwater. The Mediterranean is a net evaporative basin with a small net volume inflow at the Strait of Gibraltar but an overturning that is about 20× stronger, importing salinity 36.2 waters and exporting Mediterranean Overflow Water at salinity 38.4 at a depth of 1000 m (Sánchez-Román et al., 2009). In reality there is no source of salt in the Mediterranean, but as the model formulation is volume conserving, there is no net flow through the Strait of Gibraltar and the net evaporation in the model Mediterranean represents a virtual salt source. An overturning of 0.8 Sv with the aforementioned
205 salinity differences would result in a salt transport of $1.8\,\mathrm{kt\,s^{-1}}$ into the Atlantic. The model salt transports of both simulations are somewhat smaller at $1.2 \pm 0.1\,\mathrm{kt\,s^{-1}}$ which is equivalent to a freshwater transport of $0.032 \pm 0.002\,\mathrm{Sv}$. Through the shallow Bering Strait relatively fresh water with mean salinity of 32.5 ± 0.3 flows northward into the Arctic Ocean because of sea surface height differences between the Arctic and North Pacific (Woodgate and Aagaard, 2005).

https://doi.org/10.5194/os-2020-76
Preprint. Discussion started: 18 August 2020

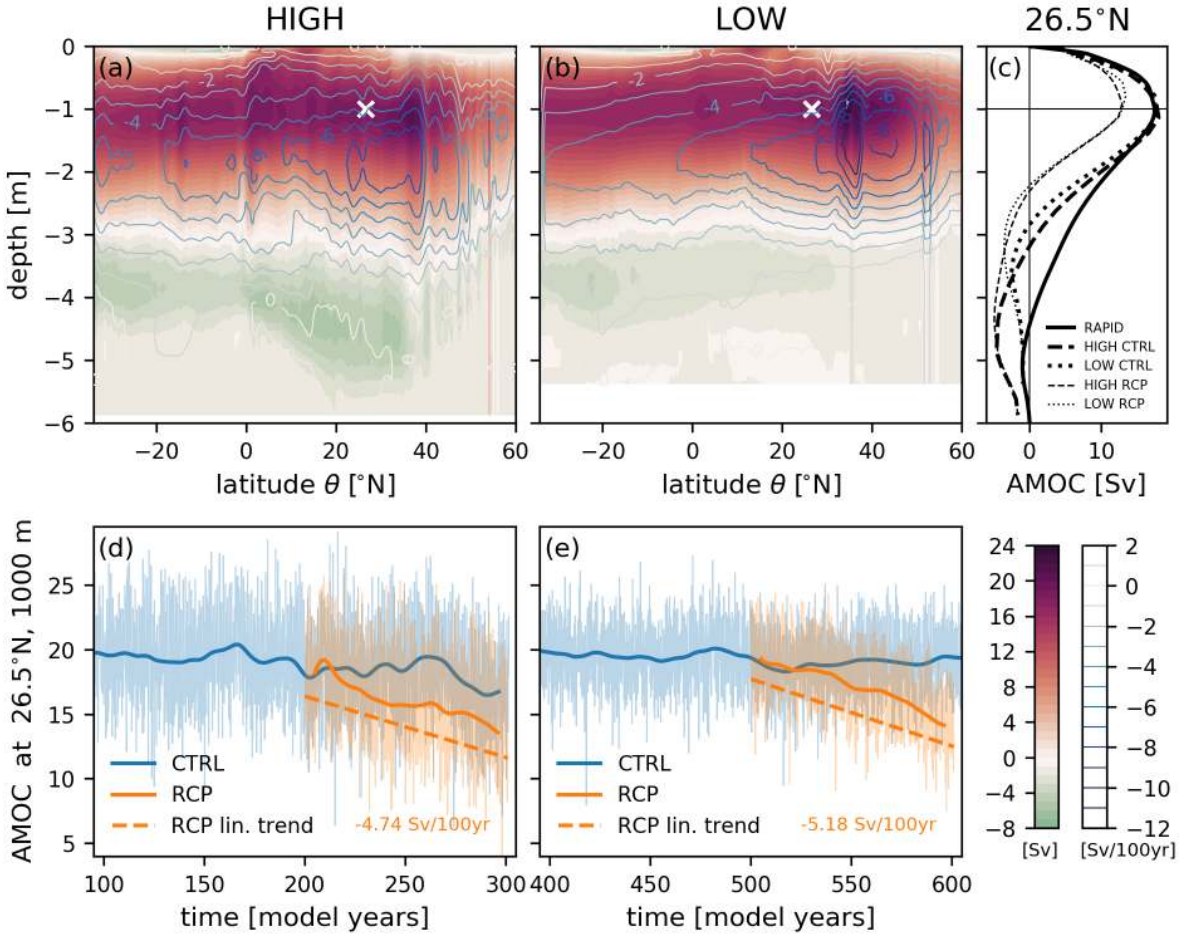

Figure 5. AMOC mean streamfunctions $\psi(\theta, z)$ of the HIGH (a) and LOW (b) CTRL simulations together with the linear trends as contour lines every 1 Sv/century. At 26.5°N and 1000 m depth, the white crosses mark the location of AMOC strength whose time evolution is depicted in (d) and(e). Panel (c) compares the modeled CTRL mean streamfunction profiles at 26.5°N (thick dashed/dotted) to the RAPID observations (solid) and also presents the changed streamfunction after 100 years in the RCP simulation (thin dashed/dotted). Monthly (thin) and 10 year lowpass filtered (thick) AMOC time series of the HIGH (d) and LOW (e) CTRL (blue) and RCP (orange) simulations. The linear trends are indicated by offset dashed lines.

https://doi.org/10.5194/os-2020-76
Preprint. Discussion started: 18 August 2020


Ocean Science Discussions

3 Results

3.1 AMOC

Figure 5 shows the meridional overturning streamfunction of the CTRL mean state (colors) together with the RCP trends (contours) in both HIGH and LOW simulations. The maximum of ψ is located just below 1 km depth for both simulations around 35°N, but the LOW upper cells stretches further north consistent with its STG that extends too far north (cf. Fig. 4). The Antarctic Bottom Water cell is stronger and extends further north in the HIGH simulation. Both simulations experience a similar weakening and shoaling trend of the upper cell and a slight strengthening of the lower cell. The HIGH latitudinal gradient in the weakening trend around the maxima at 2 km is weaker so that the HIGH AMOC weakening is stronger at 34°S but weaker in the Northern Hemisphere compared to the LOW simulation.

The evolution of the AMOC strength is measured at the latitude of the RAPID mooring array, 26.5°N, and the depth of maximum overturning, $1\,\mathrm{km}$. In contrast to the array, the streamfunction in Fig 5 contains (negligible) contributions from the Gulf of Mexico at 26.5°N. Both simulations' CTRL mean AMOC strength compare favorably to the observations with approximately $18\,\mathrm{Sv}$ and they respond with a similar linear weakening trend of $4.7\,\mathrm{Sv/century}$ and $5.2\,\mathrm{Sv/century}$ to the RCP forcing, respectively. Due to the presence of an eddying ocean (HIGH), the monthly variability (thin line) is larger than in LOW.

3.2 Surface freshwater fluxes

The Atlantic is a net evaporative basin and Fig. 6 shows maps of the total surface freshwater flux, F_{surf}, and its major contributing components: precipitation P and evaporation E. In addition, F_{surf} comprises runoff from land R and ice, as well as sea ice melt and brine rejection which, from here on, are all defined as positive freshwater fluxes into the ocean. Precipitation occurs mainly in the ITCZ region, with stronger maxima in the HIGH simulation over the Gulf Stream, and in the midlatitude storm tracks. In the HIGH (LOW) CTRL simulation between 34°S and 60°N there is a net freshwater loss of 0.88 (0.93) Sv. Evaporation is strongly tied to SSTs (Fig. 1) with most occurring in the subtropical gyres and at the above zonal-average SSTs of the western boundary currents and their extensions. Runoff occurs from all coasts bordering the Atlantic and is distributed over larger areas surrounding the river mouths in the model which is visible on the total freshwater flux subplots of Fig. 6.

The forced freshwater flux trends in Fig. 6 reveal the general intensification of the hydrological cycle as SSTs generally increase (Fig. 1). Linear trends of -0.14 (-0.16) Sv/century between 34°S and 60°N in the HIGH (LOW) RCP intensify the Atlantic's evaporative nature. The notable exception to this global trend in both simulations is the subpolar gyre where SSTs decline which results in less evaporation and hence a larger net freshwater flux into the ocean. This reduction in evaporation in the SPG is more pronounced in the HIGH simulation compared to the LOW simulation. Regional differences between the simulations include smaller positive trends along the US East coast due to the different Gulf Stream separation behavior and the related southward extent of the subpolar gyre. The runoff into the Atlantic and Arctic increases almost everywhere, except for rivers from South America. The trends of the surface freshwater flux components are similar on a large scale between HIGH and LOW (see Fig. 9).

https://doi.org/10.5194/os-2020-76
Preprint. Discussion started: 18 August 2020

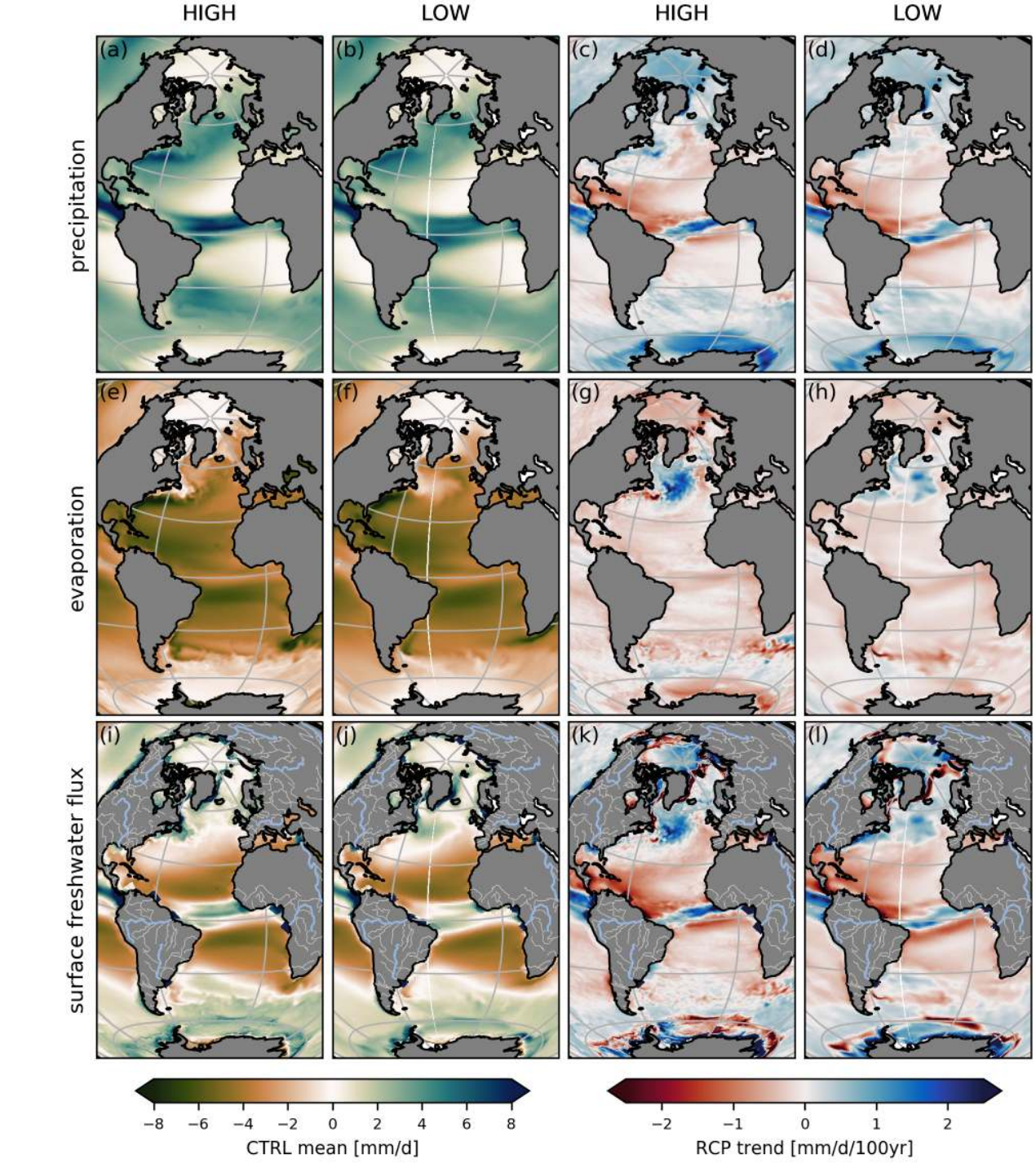

Figure 6. The simulated surface freshwater flux F_{surf} (bottom row) and its main components, precipitation P (top) and evaporation E (middle). The means of the HIGH (left column) and LOW (center left) CTRL simulation and the linear trends of the HIGH (center right) and LOW (right) RCP simulations.

https://doi.org/10.5194/os-2020-76
Preprint. Discussion started: 18 August 2020

Ocean Science
Discussions
Open Access
EGU

3.3 Meridional transport of freshwater

We decompose the meridional freshwater transport into different terms related to the overturning and azonal gyre circulation as well as an eddy component (equations in Appendix B). Budget term computations are performed on the original ocean model grid which leads to small differences between model zonal transects and the true parallel of a given latitude in the mid- to high-latitudes of the Northern Hemisphere.

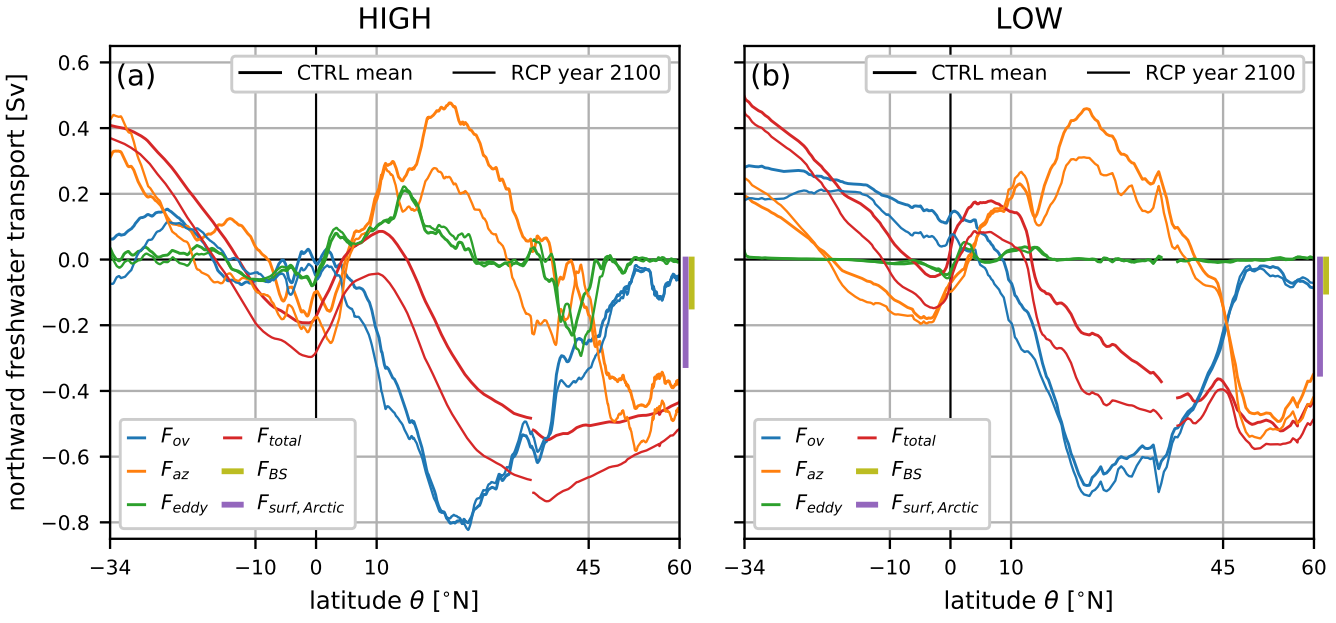

Figure 7. The meridional freshwater transports as a function of latitude θ for the HIGH (a) and LOW (b) simulations. Thick solid lines are the means of the 30 CTRL years following the branch-off point and thin lines are the year 2100 values of the linear RCP fit. The total transport terms (red) are decomposed into an overturning (blue), an azonal gyre (orange), and an eddy contribution (green). The olive vertical line to the right of subplots illustrates the Bering Strait inflow and the purple line shows the surface freshater flux in the Arctic. Around the Mediterranean inflow at 36°N the total and eddy terms are masked.

Figure 7 shows the meridional dependence of the zonally integrated total northward freshwater transport, F_{tot}, together with its different components. The figure includes both the 30 year CTRL means and the year 2100 values of the linear RCP trends. At 60°N, F_{tot} is negative because relatively fresh water is imported into the Arctic via Bering Strait (Tbl. 2). Despite different volume fluxes at Bering Strait, the freshwater inflow is about the same between the simulations because of the stronger fresh bias of the LOW simulation (cf. Tbl. 2, vertical lines in Fig. 7, Fig. 3). The Arctic is a net precipitative basin, in part due to its extensive catchment area, resulting in even more freshwater entering the Atlantic at 60°N. In the subpolar gyre and the ITCZ, i.e. in latitudes of net precipitation, freshwater diverges, while net evaporation in the subtropical gyres results in freshwater convergence by the oceanic transport. Under the RCP forcing scenario, the total freshwater flow is more southward because more freshwater enters at 60°N primarily due to increased net precipitation (including runoff) in the

https://doi.org/10.5194/os-2020-76
Preprint. Discussion started: 18 August 2020

Arctic. Generally, meridional gradients of the total transports in precipitative and evaporative latitudes increase as a result of the enhanced hydrological cycle. Notable differences between the HIGH and LOW F_{tot} are at the STG-SPG boundary at 45°N where the LOW F_{tot} does not exhibit the negative transport trend of the HIGH F_{tot}, and the meridional position of the tropical freshwater transport divergence related to the southward biased ITCZ position of the LOW simulation.

The AMOC carries both relatively salty surface waters and fresh Antarctic Intermediate Waters northward and salty North Atlantic Deep Water south. The overturning freshwater transport thus depends on the vertical distribution of the zonally averaged salinities relative to the depth of the overturning cell (cf. Figs. 3 and 5). Without changes to salinity, a weakening AMOC would reduce the overturning transport, and with a constant AMOC, the intensifying hydrological cycle would lead to enhanced meridional gradients in the transport across precipitative and evaporative parts of the ocean. With the weakening AMOC under the RCP scenario, the F_{ov} trend is negative everywhere in the LOW simulation, while the HIGH F_{ov} trend is not latitudinally coherent in its sign. The F_{ov} decrease around 40-50°N of the HIGH simulation is caused by the northward migration of the boundary between the subtropical and subpolar gyres. The decrease in the overturning transports has some of its largest expression at 34°S and the salinity stratification bias of the South Atlantic (Fig. 3j) results in a positive F_{ovS} bias which is more pronounced in the LOW compared to the HIGH simulation.

In the absence of eddies, the decomposition of the total flow into the overturning and azonal component depends on the azonality of the velocity and salinity fields. Both the North and South Atlantic subtropical gyres transport freshwater north due to their opposite zonal asymmetry in salt content near the surface (Fig. 3) while the subpolar gyre transports freshwater south. Under the climate change scenario, F_{az} generally becomes more southward north of 20°S in the STGs and the SPG. The gyre transport trends consist both of a gyre strength signal (Fig. 4) and one due to the salinity azonality trend (Fig. 8). In the HIGH simulation the F_{az} trends are the largest contribution to the total southward freshwater trends. In fact, between 20-40°N the HIGH F_{az} trend is so negative due to the strong salinification along the North American Atlantic coast (Fig. 8), that the F_{ov} trend becomes slightly positive. This occurs also around 5-20°S in the HIGH simulation where F_{az} switch signs under forcing. These negative F_{az} trends are much weaker in the LOW simulation so that the overturning component trend remains latitudinally coherent in its sign.

Eddy transports of freshwater and salt are not associated with volume fluxes as they are due to correlations between salinity and flow anomalies, which we define with a cutoff timescale of one year, i.e. including the seasonal cycle. A detailed analysis of the eddy salt transports revealed that they are associated with two distinct mechanisms (Treguier et al., 2012). First, at the equatorward edges of the STGs seasonal variations in surface salinity and wind driven circulation cause eddy transports. Second, at the boundary between the subtropical and subpolar gyres baroclinic mesoscale eddies are responsible for eddy transports. As expected, in the diffusive LOW simulation the eddy transports are negligible outside tropical seasonal variability, but in the HIGH simulation, the eddy freshwater transports F_{eddy} contribute significantly and bring freshwater polewards in the low latitudes and equatorwards around the Gulf Stream and its extension. The eddy transports thus move freshwater generally down-gradient, which is parameterized in the LOW simulation by the Gent-McWilliams scheme as a diffusive salt flux (Gent and McWilliams, 1990). Under the RCP scenario, there is essentially no change in the small eddy transports of the LOW simulation, but the HIGH eddy transport magnitude changes markedly around 45°N where the Gulf Stream shifts

https://doi.org/10.5194/os-2020-76
Preprint. Discussion started: 18 August 2020

northward (Fig. 4) and the meridional salinity gradient increases (Fig. 8). In the absence of eddy transports in LOW 45°N there is a divergence of freshwater around 40-45°N which is absent in the HIGH simulation. This LOW freshwater divergence contributes to the salinity bias (cf. Fig. 3f).

3.4 Salinity trends

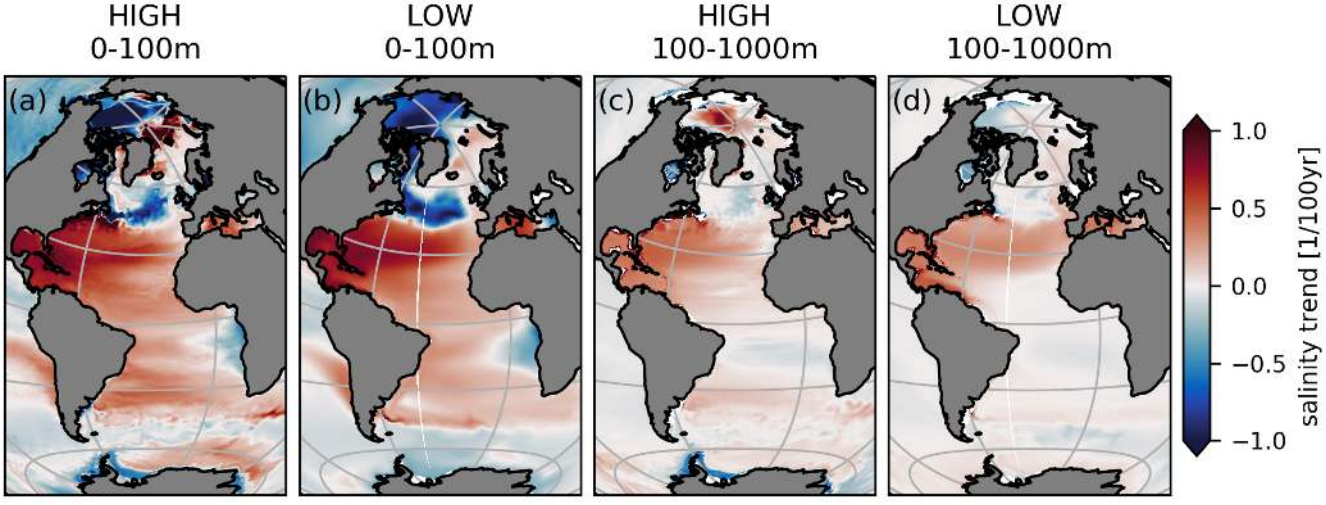

Figure 8. Linear trends of the vertically averaged salinity in the surface (0-100 m) and subsurface (100-1000 m) layers under the RCP scenario.

In our RCP climate change scenario, the Atlantic's salinity changes significantly as surface freshwater fluxes and transport convergences change, even though these salt storage changes are small compared to the fluxes and their changes. Figure 8 shows the linear trend of the vertically averaged salt content for the surface (0-100 m) and subsurface (100-1000 m) layers. In the forced salinity response the signature of the enhanced hydrological cycle is imprinted: the upper kilometer of the Atlantic south of 45°N largely salinifies, in particular in the NA-STG. Enhanced runoff from Africa decreases the salinity in the eastern SA-STG whereas decreasing runoff from South America enhances the salinification downstream of the Brazil and North Brazil Currents (see Fig. 6). While the subpolar gyre freshens uniformly in LOW, this is only the case for the eastern HIGH SPG while it is positive in the East and West Greenland as well as Labrador Currents bringing salt into the subpolar gyre. This is the result of advection of salinifying waters from the central Arctic north of Greenland and Svalbard. While the Arctic surface layer between Bering Strait and the North Pole becomes fresher in both simulations due to enhanced net precipitation including runoff, the subsurface salinifies strongly in the HIGH simulation enhancing stratification.

The zonal gradient of the salinity trends of the upper 1000 m in Fig. 8 is generally westward equatorward of 45° and more pronounced in the HIGH simulation. This leads to more azonal northward salt and southward freshwater transport by the North Atlantic subtropical gyre and where the southward Angola Current carries runoff from tropical Africa southward.

https://doi.org/10.5194/os-2020-76
Preprint. Discussion started: 18 August 2020


Ocean Science
Discussions
Open Access
EGU

South of 25°S the trend enhances the existing zonal salinity gradient resulting in strengthened azonal transport components (Fig. 7). The azonality at 34°S is opposed by surface freshwater flux trends at this latitude. This is more strongly so in the LOW simulation compared to the HIGH simulation (Fig. 6) where it leads to a weaker enhancement of the azonal transport components.

3.5 Freshwater budget

In order to gain insight into regional changes, we evaluate the freshwater budget over several regions of the Atlantic and Arctic, which is formulated as

$$\frac{\mathrm{d}\bar{W}}{\mathrm{d}t} = F_\nabla + F_{surf} + F_{mix} \tag{1}$$

where the change in freshwater storage over time $\mathrm{d}\bar{W}/\mathrm{d}t$ over a region is a consequence of the freshwater convergence across the lateral volume boundaries F_∇, surface fluxes F_{surf}, and a residual mixing term F_{mix} that captures subgridscale diffusion (including eddy parametrizations) and errors introduced by our choice of the reference salinity $S_0 = 35$. The freshwater content W of a volume V of ocean water is defined relative to the reference salinity as $\bar{W} = -1/S_0 \int (S - S_0)\,\mathrm{d}V$. Similarly, freshwater transport across a surface is defined as $F = -\int \frac{S-S_0}{S_0} \boldsymbol{u}_\perp \,\mathrm{d}A$ where $\boldsymbol{u}_\perp$ is the velocity perpendicular to the durface element $\mathrm{d}A$. Surface freshwater fluxes, F_{surf}, are implemented as virtual salt fluxes, F^S_{surf}, in the POP2 model and we calculate this flux as $F_{surf} = -F^S_{surf}/S_0$.

Figure 9 presents the freshwater and salt budget terms for each of the regions and the Atlantic from 34°S to 60°N as a whole. Panel (a) is a summary of the tendency and main freshwater flux terms into the ocean and panel (b) presents the constituent components in more detail. The mean values of the CTRL simulations are represented by bars and the 100 year linear trends by arrows. The summary plots show how the subtropical gyres are net evaporative and ocean currents converge freshwater there. Both the ITCZ and the subpolar gyre gain freshwater through surface fluxes. Here the freshwater transport divergence is much smaller in magnitude compared to the STG freshwater convergences both due the smaller areas and flux densities (cf. Figs. 1 and 6i/j) and the STGs dominate the signal of the whole Atlantic from 34°S to 60°N. The freshwater reservoir tendency term, $\mathrm{d}\bar{W}/\mathrm{d}t$, is small compared to the other terms. However, for example for the whole Atlantic between 34°S and 60°N, the tendency term is crucial in closing the budget as the trends of the transport convergence, $-\nabla F_{tot}$, are smaller than the opposing trends in the surface fluxes. Full depth regionally integrated salt content trends are very similar between the simulations with largest salt content increase in the NA-STG (cf. Figs. 9a and 8). The mixing term is negligible in the HIGH simulation and sizable in the LOW simulation as it includes the parameterized diffusion by eddy fluxes which act down-gradient, thus adding freshwater to the saltier, evaporative STGs.

The detailed plot (9b) contains the major surface freshwater flux terms as well as the meridional transport components. As discussed with the surface flux maps (Fig. 6), both the means of the CTRL simulations (bars) and the RCP trends (arrows) are similar between the simulations given that the exact numbers depend on the choice of bounding latitude. South of 45°N, all chosen regions experience more evaporation than precipitation (Fig. 6), but in the ITCZ there is net freshwater flux into the ocean due to a large runoff especially from the Amazon and Congo rivers. The strongest trends exists in the NA-STG,

https://doi.org/10.5194/os-2020-76
Preprint. Discussion started: 18 August 2020

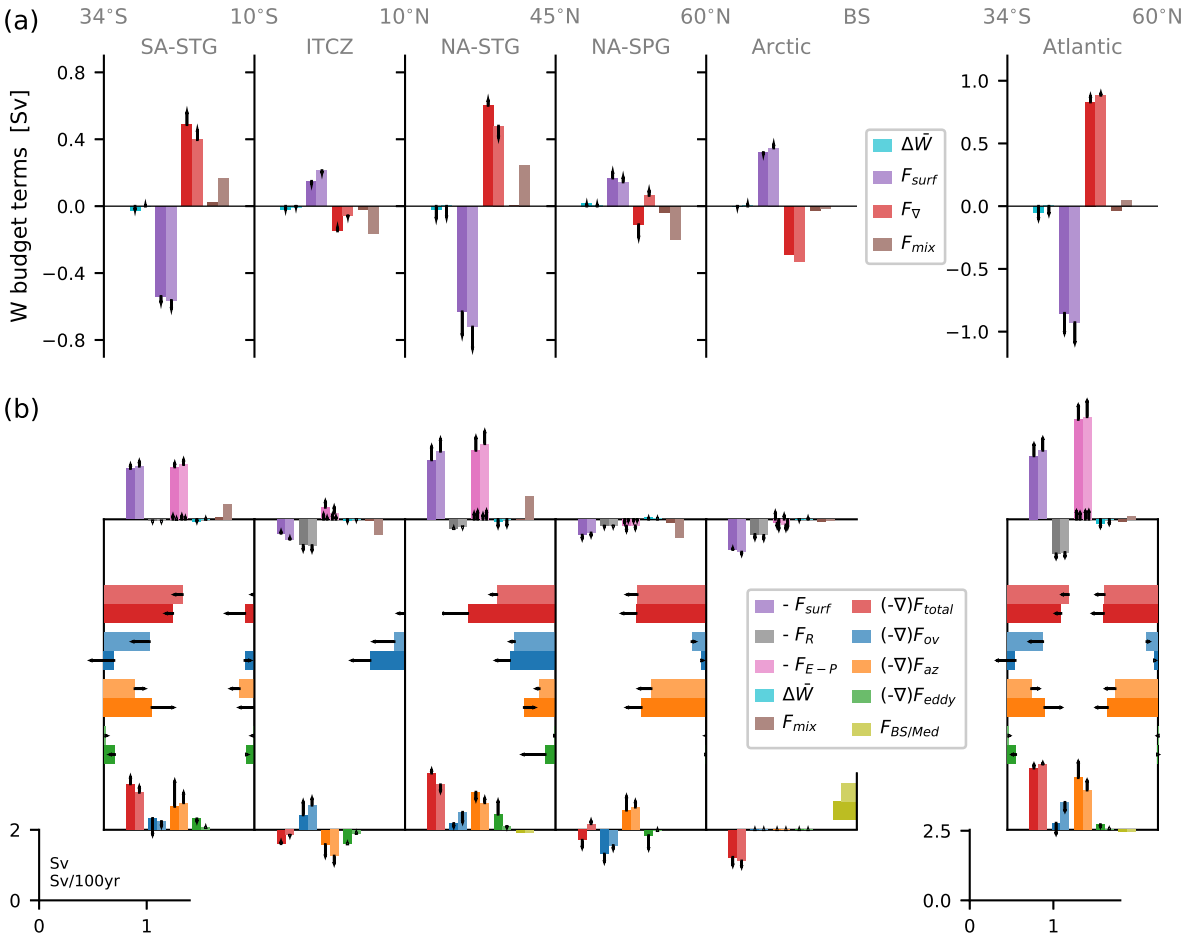

Figure 9. Integrated freshwater budget (Eq. 1) for different zonal bands of the Atlantic with the boundary latitudes indicated at the top in grey and shown in Fig. 1. Bars are the CTRL simulation averages and arrows indicate the linear change in year 2100 of the RCP simulations. Panel (a) summarizes the freshwater budget for the regions with the terms of Eq. (1) with darker (lighter) colors representing the HIGH (LOW) simulation. The notation is explained in Appendix B and $\Delta\bar{W}$ is the change in freshwater content, over 30 years of the CTRL simulations and 100 years of the RCP simulations. Panel (b) shows the freshwater budget terms in detail where the horizontal bars are advective transports across the meridional boundaries with their convergence indicated by the vertical bars at the bottom. In addition the inflow from the Bering Strait ('BS') and the Mediterranean ('Med'). The bars at the top represent atmospheric fluxes, the freshwater content change over time, as well as the mixing term and all bars are oriented such that inward pointing bars indicate addition of freshwater. The two additional arrows at the zero line of the P+E surface flux bars are the trends of the precipitation (right) and evaporation (left) separately. Note that the vertical scale of the top and bottom bars is identical, but the horizontal scales is different; as are the scales for the regions (left of the legend) and the whole Atlantic (to the right of the legend).

https://doi.org/10.5194/os-2020-76
Preprint. Discussion started: 18 August 2020

but marked differences between the simulations' freshwater input trends exist only in the mid and high latitudes. In the SPG the HIGH input increases by 32% in contrast to the LOW increase of 18%, mainly due to a stronger reduction in evaporation because of the lower SST trends (Fig. 1). In the Arctic the HIGH input increases by 22% from 0.35 Sv to 0.42 Sv, as opposed to the LOW simulation's 5.7% increase from from 0.35 Sv to 0.37 Sv, mainly due to different sea ice fluxes (not shown).

In steady state, the oceanic freshwater convergence compensates the surface fluxes. The barotropic and hence total salt transports is southward everywhere due to the import through Bering Strait which is larger in the HIGH simulation, while the barotropic freshwater transport term sign and magnitude depends on the choice of S_0 (Schauer and Losch, 2019). The magnitude of these regional convergences shown in red in Fig. 9a and as vertical bars on the bottom axis in Fig. 9b is generally smaller for the LOW simulation compared to the HIGH simulation. The HIGH and LOW decomposition differences into overturning and azonal convergence offset each other in the STGs, the ITCZ, and the Atlantic as a whole, resulting in the same sign of the total transport convergence. Only in the SPG does the sign of the total convergence differ as the overturning convergence is stronger and the azonal divergence is weaker in the HIGH simulation and the mixing term captures the parametrized eddy transports in the LOW simulation. The extreme strengthening of the HIGH eddy transport at 45°N is related to the northward shift of the Gulf Stream under forcing (cf. Fig. 7). The trends in the overturning and azonal convergence trends offset each other (except in the HIGH NA-STG with its strong growth in eddy convergence) indicating a change in the azonality of the salinity distribution (cf. Fig. 8).

3.6 AMOC stability indicators

The freshwater import (export) by the AMOC constitutes a negative (positive) feedback. The freshwater convergence by the overturning circulation $\Sigma = F_{ovS} - F_{ovN}$, where F_{ovS}/F_{ovN} are located at 34°S/60°N, has been suggested as an indicator for an AMOC multiple equilibrium regime (Dijkstra, 2007; Huisman et al., 2010). Figure 10 shows the evolution of these indicators together with the azonal freshwater transport at 34°S, F_{azS}, for both CTRL and RCP simulations. Both the HIGH and LOW CTRL simulation initially equilibrate with increasing F_{ovS} values. At the point where the RCP simulations are branched off, F_{ovS} appears to have reached an equilibrium as the concurrent CTRL time series are statistically stationary. Despite a very similar overturning strength, the LOW CTRL F_{ovS} values are significantly higher due to the stronger vertical salt bias (Fig. 3). Non-eddying CMIP5 models have a positive bias in the F_{ovS} sign and may hence be too stable; much of this bias is a result of the salinity bias with fresh surface anomalies south of 20°N and salty anomalies elsewhere in the Atlantic (Mecking et al., 2017). Artificially replacing the CMIP5 model salinities by observed values as in (Mecking et al., 2017), reduces F_{ovS} to negative values. The CTRL azonal component F_{azS} equilibrates faster than the overturning component as it relates to the shallower transport by the wind-driven STGs. The total freshwater transport at 60°N is almost identical between the simulations and consists predominantly of the azonal component (cf. Figs. 7, 9), but the exact azonal vs. overturning decomposition differs such that the LOW F_{ovN} magnitude is larger than the HIGH F_{ovN} magnitude, resulting in a larger offset in Σ.

In response to the RCP forcing, the F_{ovS} values decrease because the salinity trends offset the fresh bias near the surface (cf. Figs. 3 and 8) with the HIGH F_{ovS} trend being stronger at -0.14 Sv/century compared to the LOW trend at -0.10 Sv/century. The Σ value is also plotted in Fig. 10 as well and its trend is evidently dominated by F_{ovS} while F_{ovN} barely changes under

https://doi.org/10.5194/os-2020-76
Preprint. Discussion started: 18 August 2020

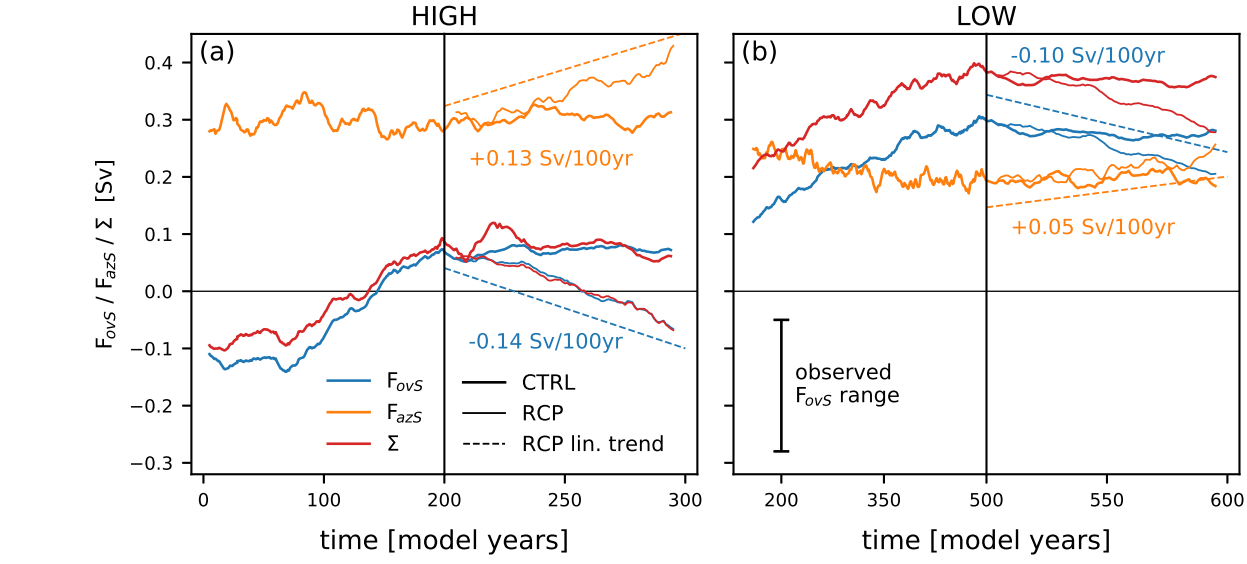

Figure 10. Time series of the annually averaged freshwater import into the Atlantic by the overturning circulation F_{ovS} at 34°S (blue), the azonal freshwater transport contribution F_{az} (orange), and the overturning divergence between 34°S and 60°N, Σ (red). All available data is shown of the CTRL simulations (thick solid) together with the RCP simulations (thin solid) and their offset linear trends (thin dashed). The observed F_{ovS} range is from Weijer et al. (2019). Note the different time scales left and right of the RCP branch-off points in the middle of the time axis.

forcing (Fig. 7). The azonal gyre component F_{azS} also evolves in response to the forcing (cf. Fig. 8) and is connected to F_{ovS} through the overall freshwater budget (Cimatoribus et al., 2012). Its change compensates the change in F_{ovS} completely in the HIGH simulation and only half of it in the LOW simulation. Both F_{ovS} and Σ indicate a shift into the multiple equilibrium regime under the RCP forcing in the HIGH but not the LOW simulation.

4 Summary and Discussion

We compared the Atlantic freshwater budget between strongly eddying (HIGH) and coarse resolution (LOW) simulations with the CESM under a present day control forcing (CTRL) and a climate change scenario with increasing greenhouse gases (RCP). Previous studies have analysed the Atlantic freshwater budget's present day state with strongly eddying ocean models (Treguier et al., 2012) or investigated the freshwater budget under climate change but with coarse resolution ocean models (Drijfhout et al., 2011), but this is the first analysis of the freshwater budget under climate change investigating the effect of strongly eddying oceans. Apart from the ocean horizontal resolution in the CESM, also the atmosphere model component version and resolution differ. However, the mean surface freshwater fluxes are comparable where ocean biases are comparable and the forced hydrological cycle response is similar between the HIGH and LOW simulation (Fig. 6). In validating the simulations, uncertainty in observations, particularly in the different $P-E$ products (Fig. 2), must be acknowledged (Trenberth et al.,

https://doi.org/10.5194/os-2020-76
Preprint. Discussion started: 18 August 2020

2011). A multidecadal variability signal, significant with respect to a red noise null hypothesis, also exists in the CESM HIGH simulation (Jüling et al., 2020). This could potentially influence the results (Jüling et al., 2020), but the magnitude of the response to the strong RCP forcing is very large compared to this internal variability.

Increasing the resolution of the ocean component enables more realistic simulation of currents, eddies and overflows, and the circulation features such as the Gulf Stream separation or the Agulhas retroflection are better represented in the HIGH simulation (Fig. 4). We find that many ocean biases are reduced in the HIGH simulation compared to the LOW simulation. Although the HIGH ocean presents a more realistic boundary condition to the atmosphere with more energy at smaller spatial and temporal scales (Kirtman et al., 2012), the atmosphere freshwater flux CTRL mean and RCP trends are similar between the two model setups (cf. Figs. 2d, 6, and 9). The large scale hydrological cycle strengthens similarly with generally warming surface temperatures, the exception being the cooling NA-SPG (Fig. 6). Also the AMOC weakens similarly (Fig. 5) in both RCP simulations, such that any differences in the simulated responses are likely due to the different ocean model resolution. The mean and trend of the ocean freshwater and salt transport, its convergence, and its decomposition differ between the HIGH and LOW simulations, especially in regions of strong eddy activity (cf. Figs. 7 and 9).

By comparing the CTRL simulations against observations relevant to the freshwater budget, we find that the HIGH simulation's biases are notably reduced compared to the LOW simulation. In particular, we diagnosed reduced biases of SST (Figs. 1 and A1), the precipitation minus evaporation fluxes (Figs. 2 and A2), the 3D Atlantic salinity distribution (Figs. 3 and A3). Two phenomena contribute to the strong meridional surface salinity bias gradient of the LOW simulation that also plagues other coarse resolution models (Mecking et al., 2017): first an unrealistically large import of too fresh surface waters from the Southwest Indian Ocean into the South Atlantic (cf. Figs. 4 and A3), and second the southward shift of the ITCZ due to a more asymmetric Atlantic meridional SST bias (cf. Figs. 1 and 2).

Despite similar atmospheric changes and AMOC slowdown, there are many notable differences between the HIGH and LOW simulations. Forced circulation changes differ in that the HIGH Gulf Stream moves north and the SPG circulation strength trends show a dipole pattern as opposed to a large-scale weakening in the LOW simulation. Also, Arctic surface freshwater fluxes change differently and the sea ice response may be underestimated due to low-biased heat transport into the Arctic in the LOW simulation (Fig. 9). The large-scale structure of the F_{tot} transport is similar and so is the forced response, with the exception of the STG-SPG boundary around 45°N where the LOW simulation shows no trends in any transport component, but the HIGH simulation exhibits a large negative F_{tot} trend, due in equal parts to the eddy and overturning components. The decomposition between overturning and azonal components differs between HIGH and LOW as the azonality of both the salinity and velocity fields differ. Eddy fluxes are significant at the northern and southern boundaries of the STGs (Treguier et al., 2012, 2014).

The evolution of the AMOC under climate change is of great interest and based on our results, and that of others, simulating strongly eddying oceans does not appear to systematically influence that response (Gent, 2018; Hirschi et al., 2020). The CTRL AMOC strength and reduction under the RCP scenario are almost identical between the simulations with a reduction of $\sim 5\,\mathrm{Sv}$ from $18\,\mathrm{Sv}$ which compares well with the observed AMOC strength at the RAPID array at 26.5°N of 17.0 Sv (Smeed et al., 2018). The reduced heat transport by the AMOC into the subpolar gyre constitutes a positive atmospheric feedback

https://doi.org/10.5194/os-2020-76
Preprint. Discussion started: 18 August 2020

in that evaporation is reduced, freshening the surface in the sinking regions. The salt-advection feedback is another positive AMOC feedback and it can lead to multiple equilibria if the overturning circulation exports freshwater from the Atlantic basin. A weakened AMOC would export less freshwater which would ultimately further suppress deep water formation in the North Atlantic and vice versa. As it is not possible to prove the existence of multiple AMOC equilibria with modern coupled climate models due to the high dimensionality and the prohibitive computational cost of equilibrating the ocean circulation after millennia, it is desirable to use scalar indicators based on simpler models. The import of freshwater to the Atlantic by the overturning circulation F_{ovS} can hence provide further insight into the question of AMOC stability if atmospheric feedbacks are negligible (Huisman et al., 2010). Observations suggest a negative F_{ovS} between -0.28 and 0.05 Sv at present (Weijer et al., 2019). Due to their salinity bias at 34°S, both HIGH and LOW CTRL simulations import freshwater into the Atlantic, but this bias is significantly stronger in the LOW simulation (Figs. 3 and 10). This bias, from which all coarse resolution CMIP5 models suffer (Mecking et al., 2017; Gent, 2018), is countered by salinification of the surface under radiative forcing decreasing the F_{ovS} value which indicates decreasing stability.

The ocean mean state as well as the forced response are different with higher resolution, but from our two RCP simulations we cannot discern any systematic effect on AMOC response to climate change as it is a large-scale flow feature and the correct simulation of the sinking regions is likely more important (Hirschi et al., 2020). Yet due to the reduced salinity biases in particular at 34°S in the HIGH simulation, the indicator of the multiple equilibrium regime F_{ovS} suggest that the salt-advection feedback can destabilize the AMOC in the 21st century. However, the HIGH freshwater overturning transport response is meridionally incoherent and hence freshwater may not be simply advected northward with the AMOC. As the transport decomposition is further complicated by an eddy term, it is questionable whether the simple indicator is useful for quantifying the salt-advection feedback and it may have to be adapted. In the absence of eddy terms and changes in the salt reservoirs, the overturning and azonal components must balance which was used by de Vries (2005) to change the sign of F_{ovS}. By changing the azonality of the freshwater surface fluxes at 34°S and hence the gyre transport, Cimatoribus et al. (2012) was able to collapse the AMOC without any further changes, suggesting that also this component of the transport must be taken into account when assessing the stability. Furthermore, any interpretation of the F_{ovS} in short strongly eddy simulations should be undertaken with care. Figure 10 shows that the HIGH CTRL simulation switches sign from negative to positive F_{ovS} only after 150 years as the ocean equilibrates.

To conclude, the changes in the Atlantic freshwater and salt budgets due to global warming are fairly robust to the resolution improvement from a diffusive to a strongly eddying ocean in CESM. This strengthens trust in using the current generation of coupled climate models (CMIP5, CMIP6) and their AMOC change projections, which are computationally significantly cheaper to perform. On the other hand, the biases in the present-day state are strongly reduced in the strongly eddying ocean version of CESM and hence indicate that better parameterizations are needed in the CMIP5/CMIP6 models to reduce these biases. This reduction can be crucial for assessing the probability of tipping of the AMOC under future climate change.

https://doi.org/10.5194/os-2020-76
Preprint. Discussion started: 18 August 2020

Ocean Science
Discussions
Open Access
EGU

Appendix A: Additional Model-Observation comparison

In this appendix, we present a model-observation comparison for several other variables. Regarding the SST bias world map (Fig. A1), in the HIGH simulation warm biases are located in the high latitudes and the tropical Indo-Pacific and cold biases in the Indo-Pacific subtropical gyres and the tropical and subtropical Atlantic. The LOW SST bias is more asymmetric about the equator with large-scale cold biases only in the Northern Hemisphere subtropical gyres and the southern edge of the NA-SPG.

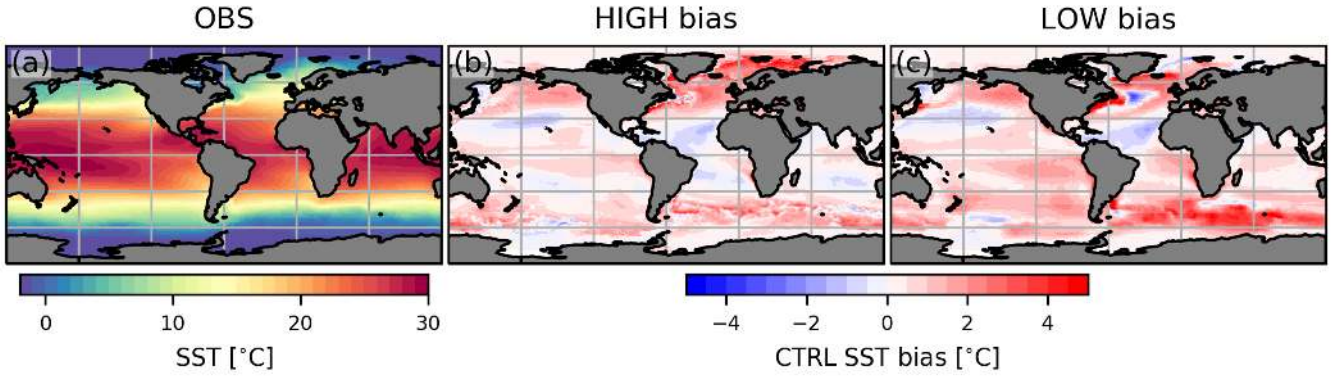

Figure A1. Bias of annual SSTs of the HIGH (left) and LOW (right) CTRL simulations, like Fig. 1.

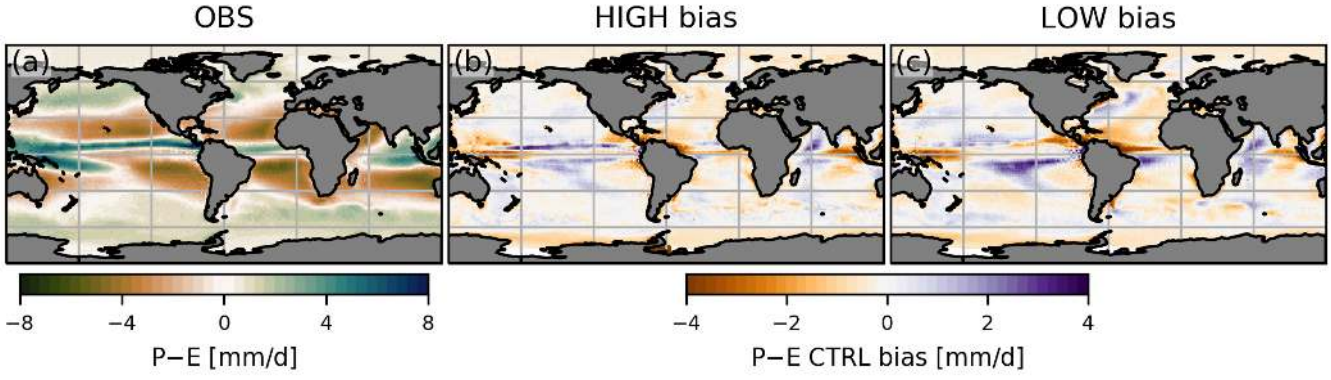

Figure A2. Comparing HIGH (left) and LOW (right) precipitation to ERA-Interim, like Fig. 2.

Appendix B: Budget calculation

As Schauer and Losch (2019) point out, the values of the freshwater flux terms are non-linearly dependent on the chosen reference salinity S_0. Traditionally, the AMOC bistability question with respect to the salt advection feedback has been framed in terms of freshwater import due to the meridional overturning.

https://doi.org/10.5194/os-2020-76
Preprint. Discussion started: 18 August 2020

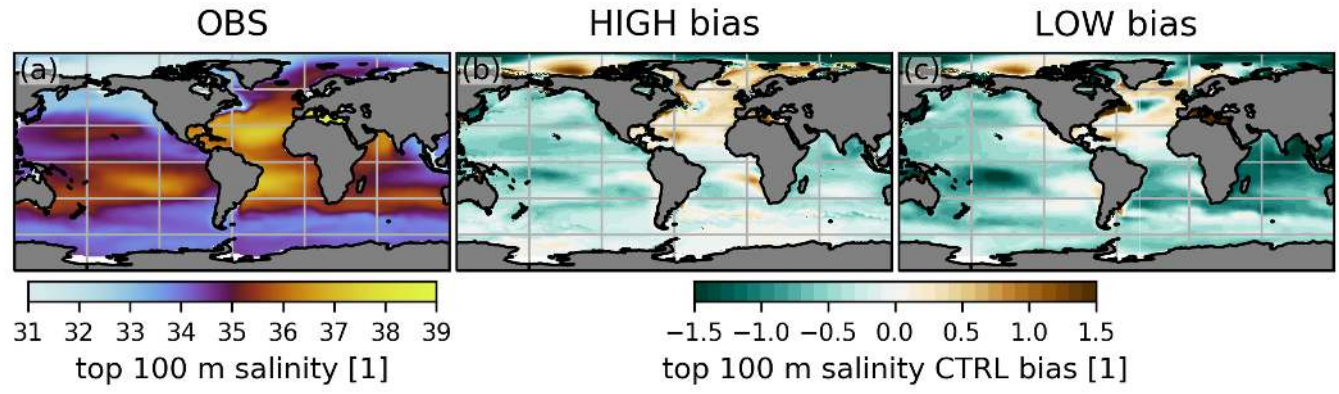

Figure A3. The salinity bias of the upper 100 m, like Fig. 3.

B1 Freshwater budget

We define freshwater fluxes in the ocean relative to a reference salinity of $S_0 = 35$ in units of $1\,\mathrm{Sv} = 10^6\,\mathrm{m}^3\,\mathrm{s}^{-1}$. The freshwater flux budget of an arbitrary full depth ocean volume is given by Eq. (1) which we repeat here for a self-contained presentation of the budget calculations:

$$\frac{\mathrm{d}\bar{W}}{\mathrm{d}t} = F_\nabla + F_{surf} + F_{mix}$$

where $\bar{W} = -\frac{1}{S_0}\int\int\int S - S_0\,\mathrm{d}V$ is the freshwater content of the volume V. The first term on the right hand side, F_∇, is due to the advection of freshwater gradients across the vertical boundary b, which is full depth and encloses the volume V:

$$F_\nabla = \int\int \boldsymbol{u}\cdot\nabla W\,\mathrm{d}b \Big/ \int\int \mathrm{d}b \tag{B1}$$

The second term is the freshwater flux at the surface comprising precipitation P, evaporation E, runoff from land R and ice I, as well as sea ice melt M and brine rejection B which are all defined as positive freshwater fluxes into the ocean:

$$F_{surf} = P + E + R + I + M + B \tag{B2}$$

The last term, F_{mix}, captures diffusion (including eddy parametrizations), errors introduced by the time averaging of the output and the choice of the reference salinity S_0 and is calculated as a residual:

$$F_{mix} = \frac{\mathrm{d}\bar{W}}{\mathrm{d}t} - F_{surf} - F_\nabla \tag{B3}$$

Furthermore, we ignore changes in sea surface height in the calculation of $\bar{W}$ such that these small effects are included in F_{mix}.

To ascertain whether a perturbation in the overturning is amplified or damped through the salt advection feedback, the freshwater transport due to the overturning is evaluated at the southern boundary (F_{ovS}). In general, the advective term can be

https://doi.org/10.5194/os-2020-76
Preprint. Discussion started: 18 August 2020

divided into a barotropic component F_{bt}, an overturning component F_{ov}, an azonal component due to the gyre circulation F_{az}, and an eddy component F_{eddy} such that:

$$F_\nabla = (F_{bt} + F_{ov} + F_{az} + F_{eddy})\big|_{y=\theta_S}^{\theta_N} \tag{B4}$$

$$F_{bt}(y) = -\hat{v}\frac{\hat{S} - S_0}{S_0} \tag{B5}$$

$$F_{ov}(y) = -\frac{1}{S_0}\int \left[\int_W^E v^* \,\mathrm{d}x\right] [\langle S\rangle - S_0]\,\mathrm{d}z \tag{B6}$$

$$F_{az}(y) = -\frac{1}{S_0}\int_{-H}^{z}\int_W^E v' S' \,\mathrm{d}x\,\mathrm{d}z \tag{B7}$$

$$F_{eddy}(y) = -\frac{1}{S_0}\int_{-H}^{z}\int_W^E \left(\overline{v\,[S - S_0]} - \overline{v}\times\overline{S}\right)\mathrm{d}x\,\mathrm{d}z \tag{B8}$$

where F_∇ is evaluated between the Southern and Northern boundaries, $\theta_{S/N}$. The hat notation $\hat{q}$ of an arbitrary quantity q denotes the section average, $\hat{q} = \int\int q\,\mathrm{d}x\,\mathrm{d}z / \int\int \mathrm{d}x\,\mathrm{d}z$. In case $q = v$, $\hat{v}$ is the barotropic velocity and $v^* = v - \hat{v}$ is the baroclinic velocity. Angled brackets $\langle q\rangle = \int q\,\mathrm{d}x / \int \mathrm{d}x$ denote zonal averaging, while primed quantities $q' = q - \langle q\rangle$ are deviations from zonal means.

In specific case of the Atlantic-Arctic freshwater budget, the oceanic advection term can be decomposed into advective freshwater fluxes at a Southern and Northern boundary, usually at the latitudes of Cape Agulhas at 34°S and Bering Strait at 68°N (F_{BS}), plus the the Mediterranean inflow (F_{Med}).

$$F_{Med} = -\frac{1}{S_0}\int_{-H}^{z}\int_{\theta_{Med,S}}^{\theta_{Med,N}} \overline{u(S - S_0)}(x = 5.5°W)\,\mathrm{d}z\,\mathrm{d}y \tag{B9}$$

where u is the zonal velocity.

Note that sometimes F_{ov} is defined to include the barotropic component (e.g. de Vries (2005)):

$$F_{ov} = -\frac{1}{S_0}\int \overline{v}\,[\langle S\rangle - S_0]\;\mathrm{d}z \tag{B10}$$

Equations (B6) and (B10) are equal if the reference salinity is equal to the section average, $S_0 = \hat{S}$, and the barotropic transport is zero, $F_{bt} = 0$.

Due to the volume-conserving, virtual salt flux formulation of the ocean model, the barotropic meridional volume transport throughout the Atlantic equals that through Bering Strait (Table 2). The barotropic freshwater transport thus depends only on the section average salinity which is so close to the reference salinity, $S_0 \approx \hat{S}$, that F_{bt} is negligibly small compared to the other transport components and hence not shown.

https://doi.org/10.5194/os-2020-76
Preprint. Discussion started: 18 August 2020

Ocean Science
Discussions
Open Access
EGU

B2 Eddy-mean decomposition

To calculate the eddy terms, we use the eddy-mean decomposition of the total flux:

$$\overline{xy} = \bar{x}\bar{y} + \overline{x'y'} \tag{B11}$$

where the overbar $\overline{x}$ denotes a time average, which we choose to be annual, and primed quantities x' denote eddy terms.

Neither the total nor the eddy freshwater transport terms, $\overline{v\,[S - S_0]}$ and $-\frac{1}{S_0}\overline{v'\,[S - S_0]'}$, are part of the model output. However, the total salt transport $\overline{vS}$ is, so that one can calculate the eddy salt transport:

$$F^S_{eddy} = \int_{-H}^{z}\int_{W}^{E} \overline{vS} - \overline{v} \times \overline{S}\,\mathrm{d}x\,\mathrm{d}z \tag{B12}$$

The freshwater eddy transport is linearly related to the eddy salt transport

$$F_{eddy} = -\frac{1}{S_0}\overline{v'\,[S - S_0]'} = -\frac{1}{S_0}\overline{v'S'} = -\frac{1}{S_0}F^S_{eddy} \tag{B13}$$

and the total freshwater flux is thus:

$$F_{total} = F_{bt} + F_{ov} + F_{az} + F_{eddy} \tag{B14}$$

Code and data availability. The analysis scripts are available at *[zenodo link to final code repository]*, while the model output is stored at SURFsara and available upon request to the corresponding author.

Author contributions. AJ, AvdH, DC, and HD conceived the presented ideas in this study. AJ performed the analysis and wrote the manuscript. XZ carried out initial analysis. AvdH, DC and HD contributed to writing the paper.

Competing interests. The authors declare no competing interests.

Acknowledgements. This work was carried out under the program of the Netherlands Earth System Science Centre (NESSC), financially supported by the Ministry of Education, Culture and Science (OCW) (Grantnr. 024.002.001). This project is TiPES contribution *#xx*: This project has received funding from the European Union's Horizon 2020 research and innovation programme under grant agreement No 820970. AJ has been fully supported by NESSC, AvdH and HD in part by NESSC and in part by TiPES. The computations were performed on the Cartesius high performance computer at SURFsara in Amsterdam. Use of the Cartesius computing facilities was sponsored by the Netherlands Science Foundation (NWO) under the project 15502. We thank Michael Kliphuis (IMAU) for carrying out the CESM simulations.

https://doi.org/10.5194/os-2020-76
Preprint. Discussion started: 18 August 2020

References

Brunnabend, S. E. and Dijkstra, H. A.: Asymmetric response of the Atlantic Meridional Ocean Circulation to freshwater anomalies in a strongly-eddying global ocean model, Tellus, Series A: Dynamic Meteorology and Oceanography, 69, 1–15, https://doi.org/10.1080/16000870.2017.1299283, http://dx.doi.org/10.1080/16000870.2017.1299283, 2017.

Caesar, L., Rahmstorf, S., Robinson, A., Feulner, G., and Saba, V.: Observed fingerprint of a weakening Atlantic Ocean overturning circulation, Nature, 556, 191–196, https://doi.org/10.1038/s41586-018-0006-5, http://www.nature.com/articles/s41586-018-0006-5, 2018.

Cheng, W., Chiang, J. C., and Zhang, D.: Atlantic meridional overturning circulation (AMOC) in CMIP5 Models: RCP and historical simulations, Journal of Climate, 26, 7187–7197, https://doi.org/10.1175/JCLI-D-12-00496.1, 2013.

Cimatoribus, A. A., Drijfhout, S. S., den Toom, M., and Dijkstra, H. A.: Sensitivity of the Atlantic meridional overturning circulation to South Atlantic freshwater anomalies, Climate Dynamics, 39, 2291–2306, https://doi.org/10.1007/s00382-012-1292-5, 2012.

de Vries, P.: The Atlantic freshwater budget as a diagnostic for the existence of a stable shut down of the meridional overturning circulation, Geophysical Research Letters, 32, L09 606, https://doi.org/10.1029/2004GL021450, 2005.

Dee, D. P., Uppala, S. M., Simmons, A. J., Berrisford, P., Poli, P., Kobayashi, S., Andrae, U., Balmaseda, M. A., Balsamo, G., Bauer, P., Bechtold, P., Beljaars, A. C. M., van de Berg, L., Bidlot, J., Bormann, N., Delsol, C., Dragani, R., Fuentes, M., Geer, A. J., Haimberger, L., Healy, S. B., Hersbach, H., Hólm, E. V., Isaksen, L., Kållberg, P., Köhler, M., Matricardi, M., McNally, A. P., Monge-Sanz, B. M., Morcrette, J.-J., Park, B.-K., Peubey, C., de Rosnay, P., Tavolato, C., Thépaut, J.-N., and Vitart, F.: The ERA-Interim reanalysis: configuration and performance of the data assimilation system, Quarterly Journal of the Royal Meteorological Society, 137, 553–597, https://doi.org/10.1002/qj.828, 2011.

den Toom, M., Dijkstra, H. A., Weijer, W., Hecht, M. W., Maltrud, M. E., and van Sebille, E.: Response of a Strongly Eddying Global Ocean to North Atlantic Freshwater Perturbations, Journal of Physical Oceanography, 44, 464–481, https://doi.org/10.1175/JPO-D-12-0155.1, 2014.

Deshayes, J., Tréguier, A.-M., Barnier, B., Lecointre, A., Sommer, J. L., Molines, J.-M., Penduff, T., Bourdallé-Badie, R., Drillet, Y., Garric, G., Benshila, R., Madec, G., Biastoch, A., Böning, C. W., Scheinert, M., Coward, A. C., and Hirschi, J. J.: Oceanic hindcast simulations at high resolution suggest that the Atlantic MOC is bistable, Geophysical Research Letters, 40, 3069–3073, https://doi.org/10.1002/grl.50534, http://doi.wiley.com/10.1002/grl.50534, 2013.

Dijkstra, H. A.: Characterization of the multiple equilibria regime in a global ocean model, Tellus A: Dynamic Meteorology and Oceanography, 59, 695–705, https://doi.org/10.1111/j.1600-0870.2007.00267.x, 2007.

Drijfhout, S. S., Weber, S. L., and van der Swaluw, E.: The stability of the MOC as diagnosed from model projections for pre-industrial, present and future climates, Climate Dynamics, 37, 1575–1586, https://doi.org/10.1007/s00382-010-0930-z, 2011.

Gent, P. R.: A commentary on the Atlantic meridional overturning circulation stability in climate models, Ocean Modelling, 122, 57–66, https://doi.org/10.1016/j.ocemod.2017.12.006, 2018.

Gent, P. R. and McWilliams, J. C.: Isopycnal Mixing in Ocean Circulation Models, J. Phys. Oceanogr., 20, 150–155, https://doi.org/10.1175/1520-0485, 1990.

Good, S. A., Martin, M. J., and Rayner, N. A.: EN4: Quality controlled ocean temperature and salinity profiles and monthly objective analyses with uncertainty estimates, Journal of Geophysical Research: Oceans, 118, 6704–6716, https://doi.org/10.1002/2013JC009067, 2013.

Hallberg, R.: Using a resolution function to regulate parameterizations of oceanic mesoscale eddy effects, Ocean Modelling, 72, 92–103, https://doi.org/10.1016/j.ocemod.2013.08.007, 2013.

https://doi.org/10.5194/os-2020-76
Preprint. Discussion started: 18 August 2020

Hawkins, E., Smith, R. S., Allison, L. C., Gregory, J. M., Woollings, T. J., Pohlmann, H., and de Cuevas, B.: Bistability of the Atlantic overturning circulation in a global climate model and links to ocean freshwater transport, Geophysical Research Letters, 38, n/a–n/a, https://doi.org/10.1029/2011GL047208, 2011.

Held, I. M. and Soden, B. J.: Robust Responses of the Hydrological Cycle to Global Warming, Journal of Climate, 19, 5686–5699, https://doi.org/10.1175/JCLI3990.1, http://journals.ametsoc.org/doi/10.1175/JCLI3990.1, 2006.

Hirschi, J. J., Barnier, B., Böning, C., Biastoch, A., Blaker, A. T., Coward, A., Danilov, S., Drijfhout, S., Getzlaff, K., Griffies, S. M., Hasumi, H., Hewitt, H., Iovino, D., Kawasaki, T., Kiss, A. E., Koldunov, N., Marzocchi, A., Mecking, J. V., Moat, B., Molines, J., Myers, P. G., Penduff, T., Roberts, M., Treguier, A., Sein, D. V., Sidorenko, D., Small, J., Spence, P., Thompson, L., Weijer, W., and Xu, X.: The Atlantic meridional overturning circulation in high resolution models, Journal of Geophysical Research: Oceans, 53, 1689–1699, https://doi.org/10.1029/2019JC015522, 2020.

Huisman, S. E., den Toom, M., Dijkstra, H. A., and Drijfhout, S.: An Indicator of the Multiple Equilibria Regime of the Atlantic Meridional Overturning Circulation, Journal of Physical Oceanography, 40, 551–567, https://doi.org/10.1175/2009JPO4215.1, 2010.

Hurrell, J. W., Holland, M. M., Gent, P. R., Ghan, S., Kay, J. E., Kushner, P. J., Lamarque, J.-F., Large, W. G., Lawrence, D., Lindsay, K., Lipscomb, W. H., Long, M. C., Mahowald, N., Marsh, D. R., Neale, R. B., Rasch, P., Vavrus, S., Vertenstein, M., Bader, D., Collins, W. D., Hack, J. J., Kiehl, J., and Marshall, S.: The Community Earth System Model: A Framework for Collaborative Research, Bulletin of the American Meteorological Society, 94, 1339–1360, https://doi.org/10.1175/BAMS-D-12-00121.1, 2013.

Johns, W. E., Baringer, M. O., Beal, L. M., Cunningham, S. A., Kanzow, T., Bryden, H. L., Hirschi, J. J. M., Marotzke, J., Meinen, C. S., Shaw, B., and Curry, R.: Continuous, Array-Based Estimates of Atlantic Ocean Heat Transport at 26.5N, Journal of Climate, 24, 2429–2449, https://doi.org/10.1175/2010JCLI3997.1, 2011.

Jüling, A., von der Heydt, A. S., and Dijkstra, H. A.: Effects of mesocale ocean flows on multidecadal climate variability, 2020.

Kirtman, B. P., Bitz, C., Bryan, F., Collins, W., Dennis, J., Hearn, N., Kinter, J. L., Loft, R., Rousset, C., Siqueira, L., Stan, C., Tomas, R., and Vertenstein, M.: Impact of ocean model resolution on CCSM climate simulations, Climate Dynamics, 39, 1303–1328, https://doi.org/10.1007/s00382-012-1500-3, 2012.

Lenton, T. M., Held, H., Kriegler, E., Hall, J. W., Lucht, W., Rahmstorf, S., and Schellnhuber, H. J.: Tipping elements in the Earth's climate system, Proceedings of the National Academy of Sciences, 105, 1786–1793, https://doi.org/10.1073/pnas.0705414105, 2008.

Liu, W., Xie, S.-P., Liu, Z., and Zhu, J.: Overlooked possibility of a collapsed Atlantic Meridional Overturning Circulation in warming climate, Science Advances, 3, e1601 666, https://doi.org/10.1126/sciadv.1601666, 2017.

Lynch-Stieglitz, J.: The Atlantic Meridional Overturning Circulation and Abrupt Climate Change, Annual Review of Marine Science, 9, 83–104, https://doi.org/10.1146/annurev-marine-010816-060415, 2017.

McDonagh, E. L., Heywood, K. J., and Meredith, M. P.: On the structure, paths, and fluxes associated with Agulhas rings, Journal of Geophysical Research: Oceans, 104, 21 007–21 020, https://doi.org/10.1029/1998JC900131, http://doi.wiley.com/10.1029/1998JC900131, 1999.

Mecking, J., Drijfhout, S., Jackson, L., and Andrews, M.: The effect of model bias on Atlantic freshwater transport and implications for AMOC bi-stability, Tellus A: Dynamic Meteorology and Oceanography, 69, 1299 910, https://doi.org/10.1080/16000870.2017.1299910, 2017.

Moreton, S. M., Ferreira, D., Roberts, M. J., and Hewitt, H. T.: Evaluating surface eddy properties in coupled climate simulations with 'eddy-present' and 'eddy-rich' ocean resolution, Ocean Modelling, 147, 101 567, https://doi.org/10.1016/j.ocemod.2020.101567, https://linkinghub.elsevier.com/retrieve/pii/S1463500319302823, 2020.

https://doi.org/10.5194/os-2020-76
Preprint. Discussion started: 18 August 2020

Palter, J. B.: The Role of the Gulf Stream in European Climate, Annual Review of Marine Science, 7, 113–137, https://doi.org/10.1146/annurev-marine-010814-015656, 2015.

Rahmstorf, S.: On the freshwater forcing and transport of the Atlantic thermohaline circulation, Climate Dynamics, 12, 799–811, https://doi.org/10.1007/s003820050144, 1996.

Rahmstorf, S., Crucifix, M., Ganopolski, A., Goosse, H., Kamenkovich, I., Knutti, R., Lohmann, G., Marsh, R., Mysak, L. A., Wang, Z., and Weaver, A. J.: Thermohaline circulation hysteresis: A model intercomparison, Geophysical Research Letters, 32, L23 605, https://doi.org/10.1029/2005GL023655, 2005.

Sánchez-Román, A., Sannino, G., García-Lafuente, J., Carillo, A., and Criado-Aldeanueva, F.: Transport estimates at the western section of the Strait of Gibraltar: A combined experimental and numerical modeling study, Journal of Geophysical Research: Oceans, 114, 1–15, https://doi.org/10.1029/2008JC005023, 2009.

Schauer, U. and Losch, M.: "Freshwater" in the Ocean is Not a Useful Parameter in Climate Research, Journal of Physical Oceanography, 49, 2309–2321, https://doi.org/10.1175/JPO-D-19-0102.1, 2019.

Skliris, N., Marsh, R., Mecking, J. V., and Zika, J. D.: Changing water cycle and freshwater transports in the Atlantic Ocean in observations and CMIP5 models, Climate Dynamics, 19, 2017–8976, https://doi.org/10.1007/s00382-020-05261-y, 2020.

Small, R. J., Bacmeister, J., Bailey, D., Baker, A., Bishop, S., Bryan, F., Caron, J., Dennis, J., Gent, P., Hsu, H., Jochum, M., Lawrence, D., Muñoz, E., DiNezio, P., Scheitlin, T., Tomas, R., Tribbia, J., Tseng, Y., and Vertenstein, M.: A new synoptic scale resolving global climate simulation using the Community Earth System Model, Journal of Advances in Modeling Earth Systems, 6, 1065–1094, https://doi.org/10.1002/2014MS000363, 2014.

Smeed, D. A., Josey, S. A., Beaulieu, C., Johns, W. E., Moat, B. I., Frajka-Williams, E., Rayner, D., Meinen, C. S., Baringer, M. O., Bryden, H. L., and McCarthy, G. D.: The North Atlantic Ocean Is in a State of Reduced Overturning, Geophysical Research Letters, 45, 1527–1533, https://doi.org/10.1002/2017GL076350, 2018.

Srokosz, M., Baringer, M., Bryden, H., Cunningham, S., Delworth, T., Lozier, S., Marotzke, J., and Sutton, R.: Past, Present, and Future Changes in the Atlantic Meridional Overturning Circulation, Bulletin of the American Meteorological Society, 93, 1663–1676, https://doi.org/10.1175/bams-d-11-00151.1, 2012.

Stocker, T. F., Qin, D., Plattner, G.-K., Tignor, M., Allen, S. K., Boschung, J., Nauels, A., Xia, Y., And, V. B., and P.M. Midgley (eds.): IPCC, 2013: Climate Change 2013: The Physical Science Basis. Contribution of Working Group I to the Fifth Assessment Report of the Intergovernmental Panel on Climate Change, Cambridge University Press, Cambridge, United Kingdom and New York, NY, USA, https://doi.org/10.1017/CBO9781107415324, 2013.

Stommel, H.: Thermohaline Convection with Two Stable Regimes of Flow, Tellus, 13, 224–230, https://doi.org/10.3402/tellusa.v13i2.9491, 1961.

Toom, M. D., Dijkstra, H. A., Cimatoribus, A. A., and Drijfhout, S. S.: Effect of atmospheric feedbacks on the stability of the Atlantic meridional overturning circulation, Journal of Climate, 25, 4081–4096, https://doi.org/10.1175/JCLI-D-11-00467.1, 2012.

Treguier, A. M., Deshayes, J., Lique, C., Dussin, R., and Molines, J. M.: Eddy contributions to the meridional transport of salt in the North Atlantic, Journal of Geophysical Research: Oceans, 117, 1–19, https://doi.org/10.1029/2012JC007927, 2012.

Treguier, A. M., Deshayes, J., Le Sommer, J., Lique, C., Madec, G., Penduff, T., Molines, J. M., Barnier, B., Bourdalle-Badie, R., and Talandier, C.: Meridional transport of salt in the global ocean from an eddy-resolving model, Ocean Science, 10, 243–255, https://doi.org/10.5194/os-10-243-2014, 2014.

https://doi.org/10.5194/os-2020-76
Preprint. Discussion started: 18 August 2020

Trenberth, K. E., Fasullo, J. T., and Mackaro, J.: Atmospheric moisture transports from ocean to land and global energy flows in reanalyses, Journal of Climate, 24, 4907–4924, https://doi.org/10.1175/2011JCLI4171.1, 2011.

van Westen, R. M. and Dijkstra, H. A.: Southern Ocean Origin of Multidecadal Variability in the North Brazil Current, Geophysical Research Letters, 44, 10,510–540,548, https://doi.org/10.1002/2017GL074815, http://dx.doi.org/10.1002/2017GL074815, 2017.

Weijer, W., Maltrud, M. E., Hecht, M. W., Dijkstra, H. A., and Kliphuis, M. A.: Response of the Atlantic Ocean circulation to Greenland Ice Sheet melting in a strongly-eddying ocean model, Geophysical Research Letters, 39, n/a–n/a, https://doi.org/10.1029/2012GL051611, 2012.

Weijer, W., Cheng, W., Drijfhout, S. S., Fedorov, A. V., Hu, A., Jackson, L. C., Liu, W., McDonagh, E. L., Mecking, J. V., and Zhang, J.: Stability of the Atlantic Meridional Overturning Circulation: A Review and Synthesis, Journal of Geophysical Research: Oceans, 124, 5336–5375, https://doi.org/10.1029/2019JC015083, 2019.

Winton, M., Anderson, W. G., Delworth, T. L., Griffies, S. M., Hurlin, W. J., and Rosati, A.: Has coarse ocean resolution biased simulations of transient climate sensitivity?, Geophysical Research Letters, 41, 8522–8529, https://doi.org/10.1002/2014GL061523, 2014.

Woodgate, R. A. and Aagaard, K.: Revising the Bering Strait freshwater flux into the Arctic Ocean, Geophysical Research Letters, 32, 1–4, https://doi.org/10.1029/2004GL021747, 2005.